A K_{Ca} 2.2/2.3 Opener Reverses ET-1-induced NLRP3 Activation in Hypertensive Mice Corpora Cavernosa

Fais, RS[1,2,3*]; Comerma-Steffensen, SG[2,4]; Pinilla, E[2]; Matchkov, VV[2]; Tostes RC[1]; Carneiro, FS[1]; Simonsen, U[2*]

[1] Department of Pharmacology, Ribeirao Preto Medical School, University of Sao Paulo, Ribeirao Preto-SP, Brazil; rsfais@gmail.com, rtostes@usp.br, fsilvac@usp.br

[2] Department of Biomedicine, Pulmonary and Cardiovascular Pharmacology, Aarhus University, Aarhus, Denmark; us@biomed.au.dk, vvm@biomed.au.dk

[3] Division of Pulmonary, Critical Care, and Sleep Medicine, National Jewish Health, Denver-CO, USA;

[4] Department of Biomedical Sciences/Animal Physiology, Faculty of Veterinary, Central University of Venezuela, Venezuela. simoncomerma@biomed.au.dk.

* Correspondence: US - us@biomed.au.dk, RSF - rsfais@gmail.com.

Abstract

Hypertension-induced erectile dysfunction is associated with endothelial dysfunction in the corpus cavernosum. Membrane depolarization activates the NLRP3 inflammasome, with downregulation of endothelial Ca^{2+}-activated K^+ channels type 2.3 (K_{Ca} 2.3) and upregulation of endothelin-1 (ET-1) linked to erectile dysfunction. However, underlying mechanisms remain incompletely understood. We hypothesized that activating K_{Ca} 2.2/2.3 channels reverses erectile dysfunction and ET-1-induced NLRP3 activation in hypertensive DOCA/salt mice. Hypertension was induced in mice using a DOCA/salt model, with unilaterally nephrectomized mice as controls. We measured blood pressure, intracavernous pressure (ICP), and corpus cavernosum (CC) contractility, and performed immunoblots for K_{Ca} 2.3, caspase-1, and interleukin-1β (IL-1β). DOCA/salt mice showed impaired erectile function and increased IL-1β activity and K_{Ca} 2.3 expression. Treatment with the endothelin receptor antagonist bosentan or the K_{Ca} 2.2/2.3 channel opener NS13001 reversed these dysfunctions and reduced ET-1-induced NLRP3 activation. NS13001 also restored decreased currents in endothelial cells exposed to ET-1. These findings establish that hypertension-induced erectile dysfunction involves an ET-1/membrane depolarization/NLRP3 inflammasome axis in corpus cavernosum endothelial cells, and that targeting endothelial K_{Ca}2.2/2.3 channels represents a promising therapeutic strategy to counteract erectile dysfunction.

Keywords: Erectile dysfunction; NLRP3 inflammasome; K_{Ca} 2.2/2.3, arterial hypertension.

1. Introduction

Erectile dysfunction (ED) commonly accompanies arterial hypertension and reflects systemic endothelial dysfunction. Penile erection is mediated by endothelium-dependent vasodilation within the corpus cavernosum (CC), which enhances cavernosal blood inflow and increases sinusoidal compliance [1-5]. A key endothelial mechanism underlying this response is membrane hyperpolarization mediated by small-conductance Ca^{2+}-activated K^+ channels (K_{Ca}2.x), which amplifies Ca^{2+} entry, sustains endothelial nitric oxide synthase (eNOS) activity, and promotes the release of vasodilators that relax cavernosal smooth muscle [6-8]. The K_{Ca} is a diverse group of potassium channels and are divided into small SK_{Ca} (K_{Ca}2.1, K_{Ca}2.2, and, K_{Ca}2.3), intermediate (IK_{Ca} or (K_{Ca}3.1), and large conductance Ca^{2+}-activated K^+ channels (BK_{Ca} or K_{Ca}1.1) [9].

ED is a predictor of cardiovascular disease, stroke, and perhaps all-cause mortality – through an augmentation in cardiovascular mortality and independently of traditional risk factors[10,11].The K_{Ca}2.3 channel is essential for nitric oxide (NO) signaling through endothelial NO synthase (eNOS) activation. NO produced by eNOS in the vascular bed not only mediates vasodilatation but also has anti-inflammatory functions [12,13]. The downregulation of K_{Ca}2.3 leads to endothelial dysfunction and ED, and expression and/or function of K_{Ca}2.3 channels are reduced in arterial hypertension. [6,14]

The activation of K_{Ca}2.3 reduces blood pressure[3] and improves erectile function in rats. Furthermore, KCa2.3 has an anti-inflammatory effect, mainly by inhibiting the release of proinflammatory cytokines such as interleukin (IL)-6 and tumor necrosis factor-alpha (TNF-α) and by inhibiting the migration of immune cells. Thus, K_{Ca}2.3 channel plays an essential role in the modulation of the immune system [12,13].

ET-1 is closely linked with endothelial dysfunction, mainly by the modulation of various populations of K^+ channels, such as inward-rectifying (K_{ir}), ATP-sensitive (K_{ATP}), voltage-gated (K_v), and K_{Ca} channels[6,15]. ET-1 has been shown to activate mononuclear phagocytes and to promote the release of TNF-α, IL-1β, and IL-6, thereby increasing the interaction between endothelial cells and monocytes. Moreover, a recent study showed that ET-1 activates NLRP3 via Ca^{2+}-induced ROS generation and impairs erectile function[16-18].

Membrane depolarization is thought to be involved in the activation of NLRP3[19]. Therefore, the present study hypothesized that opening $K_{Ca}2.3$ channels prevents the activation of NLRP3 and reverses ED. To address the hypothesis, studies were conducted on the effect of ET-1 and an opener of KCa 2.2/2.3 channels, NS13001, on the endothelial cell K^+ currents, and the effect of NS13001 on erectile function was examined in a DOCA/salt hypertensive mouse model.

Based on these results, this study provides a novel insight into the role of $K_{Ca}2.3$ channels in mediating the relationship between hypertension and ED, conditions that often co-exist. By revealing that ET-1-induced hypertension (DOCA/salt) impairs $K_{Ca}2.3$ function and activates the NLRP3 inflammasome, leading to vascular and ED, it uncovers a previously underexplored critical mechanism. The therapeutic potential of the $K_{Ca}2.3/K_{Ca}2.2$ channel opener NS13001 in reversing these effects is a key finding, offering a targeted approach to treat ED and hypertension. This timely research highlights potassium channels as promising therapeutic targets for inflammatory-related vascular diseases and ED.

2. Materials and Methods

2.1. Animals

10-12 weeks-old C57BL/6 (~25 g) male mice were housed in a room with controlled temperature (20 - 22°C) and on light/dark cycles of 12 hrs with free access to standard chow with 0.2% sodium (Altromin 1324, Brogaarden, Denmark) and filtered water. All experimental protocols adhered to the ARRIVE guidelines [20], followed Danish legislation of animal use for scientific procedures as described in the 'Animal Testing Act' (Consolidation Act No. 726 of 9 September 1993 as amended by Act No. 1081 of 20 December 1995) and were approved by the Danish Animal Experiments Inspectorate (permission 2019-15-0201-00009).

2.2. DOCA-Salt Hypertension and Arterial Blood Pressure Measurements

Deoxycorticosterone acetate (DOCA) -salt hypertension was induced as previously described [21]. Mice were anesthetized using isoflurane (5% for induction and 2% for maintenance) in 100% oxygen (2 L/min). Briefly, mice were unilaterally nephrectomized and deoxycorticosterone-acetate (DOCA; 1 g/Kg) silastic pellets were implanted subcutaneously in the scapular region. After the DOCA surgery, the mice received buprenorphine (0.05mg/kg every 8 hours for 24 hours). DOCA mice received water containing 1% NaCl and 0.2% KCl, for 3 weeks. Unilaterally nephrectomized control mice (UNI) received silastic pellets without DOCA and tap water. Animals received either the non-selective ET-1 antagonist bosentan [30 mg/day/kg (diluted in saline) of body weight, per gavage], NS13001 [1 mg/day/kg diluted in polyethylene glycol) of body weight, per gavage], apamin [1 mg/day/kg (diluted in saline) of body weight, subcutaneous],

116 or its respective vehicle for 11 days starting 10 days after the surgery. Systolic blood pressure
117 (SBP) was measured in mice with a tail-cuff method using a RTBP1001 blood pressure system
118 (Kent Scientific Corporation, CT).

119

120 **2.3. Isolation of corpus cavernosum (CC) strips and CC primary endothelial cells**

121 For isolation of primary endothelial cells and corpus cavernosum (CC) strips, the mouse was
122 gently placed in a transparent chamber (19 cm wide x 29 cm deep x 13 cm high) and exposed to
123 isoflurane 3% in 100% oxygen (2L/min). Once the pain reflexes disappeared, the animals were
124 decapitated. After this procedure, the CC was isolated and split into 2 strips, one was used for CC
125 contractility measurements, and the other for immunoblotting.

126

127 **2.4. Drugs and solutions**

128 Physiological Krebs-Henseleit buffer of the following composition was used: NaCl 130
129 mM, KCl 4.7 mM, KH_2PO_4 1.18 mM, $MgSO_4$•$7H_2O$ 1.17 mM, $NaHCO_3$ 14.9 mM, EDTA 0.026
130 mM, $CaCl_2$•$2H_2O$ 1.6 mM and D-glucose 5.55 mM. A high concentration of KCl buffer of the
131 following composition was used: NaCl 14 mM, KCl 120 mM, KH_2PO_4 1.18 mM, $MgSO_4$•$7H_2O$
132 1.17 mM, $NaHCO_3$ 14.9 mM, EDTA 0.026 mM, $CaCl_2$•$2H_2O$ 1.6 mM and D-glucose 5.55 mM.
133 pH in all buffers was adjusted to 7.35 before its use. The incubations were performed with ET-1
134 (100 nM, Tocris 1160; diluted in 5% BSA + 95% deionized water), MCC950 (1 μM, Cayman
135 Chemical 17510; diluted in 5% DMSO and 95% deionized water), NS13001 (100 nM,
136 ChemShuttle, CA, USA; diluted in polyethylene glycol), apamin (100 nM, Latoxan L8407; diluted

137 in deionized water). The in vivo experiments were performed with bosentan (30 mg/day/kg, Sigma
138 Aldrich 157212-55-0; diluted in saline), NS13001 (1 mg/day/kg, ChemShuttle, CA, USA; diluted
139 in polyethylene glycol), apamin (1 mg/day/kg; Latoxan L8407; diluted in saline).

140

141 **2.5. Culture of primary endothelial cells of Corpus cavernosum**

142 Endothelial cells from CC of intact C57BL/6 mice were isolated as previously described[3].
143 Briefly, a freshly isolated CC strip was placed in sterile PBS and cut into small pieces together
144 with collagenase II (400 mg ml−1, Worthington Biochemical Corporation, Lakewood, NJ, USA)
145 for 60 min at 37°C. The sampled tissue was centrifuged at 900 RPM with isolation of the pellet
146 and transferred to a coated gelatin and collagen Petri dish at 37°C. The culture media was
147 Dulbecco's Modified Eagle Medium with 1% Fungizone, 1% penicillin streptomycin, newborn
148 fetal calf serum and HEPES. When reached confluence after 1–4 days, the cells were incubated
149 with the endothelium-specific CD102 [intracellular adhesion molecule 2 (ICAM2)] rat anti-mouse
150 (diluted 1:500, BD Biosciences 553326. RRID: AB_394784) for 30 min followed by incubation
151 with Dynabeads with sheep anti-rat IgG (Life Technologies, Oslo, Norway) for 30 min at 4°C.
152 Trypsin was added to separate the cells from Petri dish and transferred to dynamag 5TM (Life
153 Technologies, Oslo, Norway) for 2 min cleaning. The pellet was dissolved and left in a coated
154 Petri dish for further cultivation in endothelial cell growth serum (Provitro AG, Berlin, Germany).
155 The endothelial cells were treated with ET-1 (4 h) in the presence of NS13001 (30 min), apamin
156 (30 min), or vehicle. After the treatment, the cells were separated for patch clamp or Western blot
157 experiments.

158

159

160 **2.6. Patch-Clamp Electrophysiology**

161 Endothelial cells were detached from Petri dish with trypsin-EDTA, washed, and patch
162 clamped using a Port-a-Patch automated system (Nanion Technologies, Munich Germany), as
163 previously described [3]. Briefly, 3–5 MΩ resistance microchips were used. Currents were
164 recorded using an extracellular solution containing (in mM): 140 NaCl, 4 KCl, 10 Glucose, 10
165 HEPES, 2 $CaCl_2$ and 1 $MgCl_2$, pH 7.3–7.4. The intracellular solution was prepared as described
166 previously (Stankevicius et al., 2011) and contained (in mM): 30 KCl, 100 K-Aspartate, 1 mM
167 $MgCl_2$, 10 mM EGTA, 3 Na_2ATP, 5 mM HEPES, and 8,5 $CaCl_2$, pH 7.2. The osmolarity of all
168 solutions was 290–320 mOsm. All voltages were corrected for calculated junction potentials
169 present between the internal and external solutions before seal formation. The K^+ currents were
170 activated by voltage steps from −140 to 140 mV in 40 mV increments for 250 ms and using a
171 holding membrane potential of −80 mV. Currents measured at a step of 100 mV were used to
172 compare the effects of the $K_{Ca}2.2/2.3$ openers or blockers used in this study. All current amplitudes
173 were expressed as current density (pA/pF) normalized to cell capacitance.

174

175 **2.7. In vivo measurements of intracavernosal pressure and mean arterial pressure**

176 Mice were anesthetized with 2% isoflurane for induction and maintained with 1.5% in 100%
177 oxygen (2 L/min) [4]. Then, the left carotid artery and right CC of each mouse were cannulated
178 for continuous monitoring of mean arterial pressure (MAP) and intracavernosal pressure (ICP),
179 respectively.

180 In the DOCA and UNI mice treated with either vehicle, bosentan, NS13001, or apamin, the
181 cavernosal nerve was electrically stimulated with silver electrodes at different frequencies (5 V,
182 1 ms pulses, and frequencies between 0.5 and 20 Hz for 60 sec stimulations) to induce changes in
183 ICP. Each frequency was followed by a 2-minute resting period. Cavernosal nerve mediates the
184 relaxation and contraction of cavernous smooth muscle, respectively, together regulating the
185 erectile function of penile tissue(Dean and Lue, 2005).

186 In intact C57BL/6 mice, the cavernosal nerve was stimulated electrically with silver
187 electrodes at 6 V, 1 ms pulse width, for 60 sec, and the frequency at 16 Hz to induce changes in
188 ICP and obtain the maximum (max) ICP/MAP. Subsequently, the cavernosal nerve was stimulated
189 at the same parameters and varying the frequency from 2 to 8 Hz to determine the 50%
190 (submaximal) of ICP/MAP for each mouse(Sobrano Fais et al., 2023). Then, we administered
191 intracavernosal NS13001 (0.1 µg/Kg), apamin (20.27 µg/Kg), or vehicle. A new submaximal
192 stimulation was performed at 3, 10, 20, and 30 minutes, and the maximal stimulation at 25 minutes.
193 A second intracavernosal administration with ET-1 (0.2492 µg/Kg) or vehicle was performed, and
194 the submaximal stimulation was performed at 3, 10, 20, and 30 minutes, and the maximal
195 stimulation at 25 minutes.

196

197 **2.8. Cavernosal tissue contractility**

198 Cavernosal strips from intact C57BL/6 mice were isolated and mounted in 10 mL-myograph
199 chambers (Danish Myo Technology, Aarhus, Denmark) containing buffer continuously bubbled
200 with a mixture of BioAir (5% CO_2 and 19.82% O_2 in nitrogen) and maintained at 37°C as
201 previously described [2]. The tissues were stretched to a resting force of 2.5 mN and allowed to

202 equilibrate for 60 min. Changes in isometric force were recorded using the PowerLab/8SP data
203 acquisition system (Chart software, version 7; ADInstruments, Colorado Springs, CO). At the end
204 of the equilibration period, phenylephrine (1 μM) was added to the organ bath to verify the
205 preparations' contractile ability.

206 The contraction was evaluated by cumulative concentration-response curves to phenylephrine
207 (1 nM to 100 μM) in CC strips. Relaxation was evaluated by constructing cumulative
208 concentration-response curves for acetylcholine (ACh) (100 pM – 3 μM; endothelium-dependent
209 relaxation) and sodium nitroprusside (SNP) (10 pM – 100 μM; NO donor) in CC strips pre-
210 contracted with phenylephrine (10 μM). To investigate neurogenic relaxations in CC strips, the
211 preparations were treated with guanethidine (30 μM) and atropine (1 μM) as previously
212 described(Simonsen et al., 2001). Then, the preparations were contracted with phenylephrine, and
213 electrical field stimulation (0.5 to 32.0 Hz) was performed.

214

215 **2.9. Immunoblotting**

216 DOCA or UNI animals received either the non-selective ET-1 antagonist bosentan [30
217 mg/day/Kg (diluted in saline) of body weight, per gavage], NLRP3 inhibitor [10 mg/day/Kg
218 (diluted in saline) of body weight, subcutaneous], NS13001 [1 mg/day/Kg diluted in polyethylene
219 glycol) of body weight, per gavage], apamin [1 mg/day/kg diluted in saline) of body weight,
220 subcutaneous], or its respective vehicle for 11 days starting 10 days after the surgery. The samples
221 for this immunoblotting experiments were obtained from mice exclusively used for
222 immunoblotting, thereby avoiding interference from in vivo or ex vivo stimulation.

223 The CC endothelial cells were obtained from health mice and treated with ET-1 (100 nM,
224 Tocris 1160; diluted in 5% BSA + 95% deionized water), MCC950 (1 μM, Cayman Chemical
225 17510; diluted in 5% DMSO and 95% deionized water), NS13001 (100 nM, ChemShuttle, CA,
226 USA; diluted in polyethylene glycol), apamin (100 nM, Latoxan L8407; diluted in deionized
227 water).

228 The isolated CC from intact C57BL/6 mice were cleaned from surrounding fat tissue and then
229 snap-frozen in liquid nitrogen for storage at -80 °C. The samples were later homogenized in a lysis
230 buffer [50 mM Tris/HCl, 150 mM NaCl, 1% Nonidet P40, 1 mM EDTA, 1 μg/ml leupeptin, 1
231 μg/ml pepstatin, 1 μg/ml aprotinin, 1 mM sodium orthovanadate, 1 mM phenylmethanesulfonyl
232 fluoride (PMSF), and 1 mM sodium fluoride] (Fais et al., 2019). Protein concentration was
233 determined by the Lowry assay. Spectra multicolor broad range protein ladder (10 to 260 KDa)
234 was used as protein standard. Aliquots with 60 μg of proteins were prepared and separated by
235 electrophoresis at 100 V for 2 hours at 4° C in 4-20% Criterion TGX Stain-Free gels (bio rad) and
236 transferred for 1 hour to a nitrocellulose membrane at 100 V at 4° C. After transfer, total protein
237 was visualized using stain-free technology by exposing the membranes to UV light. Nonspecific
238 binding sites of the membrane to the primary antibodies were blocked with 0.3% iBlock solution
239 for 1 hour at room temperature. The primary antibodies described below were incubated for 12
240 hours at 4° C, and the secondary antibodies were incubated for 1 hour at room temperature. Protein
241 bands visualization was obtained by chemiluminescence after ECL reaction (Amersham ECL
242 Prime Western Blotting Detection Reagent) and image capture was performed on ImageQuant 350
243 gel imager (GE Healthcare, Piscata Way, NJ, USA). The densitometric quantification was
244 performed by ImageJ® software. Membranes were stripped with Restore 2x Western Blot
245 Stripping Buffer (Thermo) for 30 minutes at 37° C. The densitometric quantification was

246 normalized by the total protein in the pre-stained gel. Total protein is considered a more reliable
247 control than housekeeping proteins [22-24].

248 The following antibodies were used in the study: caspase-1 (diluted 1:500, Imgenex IMG-
249 5028. RRID: AB_316670), IL-1β [diluted 1:500, NovusBio NB600-633, RRID: AB_577977],
250 KCa2.3 (diluted 1:500, NovusBio NBP3-46424. RRID: AB_3738376), β-actin (diluted 1:1000,
251 Cell Signalling 5125. RRID: AB_1903890. Total protein in each lane was used as an endogenous
252 control for normalization of all proteins. Membranes were then incubated with the following
253 secondary antibodies: goat anti-mouse IgG H&L (diluted 1:10.000, ab6789, Abcam. RRID:
254 AB_955439) and goat anti-rabbit IgG H&L (diluted 1:10.000, ab6721, Abcam. RRID:
255 AB_955447).

256

257 **2.10. Statistical analysis**

258 The declared group size is the number of mice. Statistical analysis was undertaken only for
259 experiments where each group size was at least n=5. The Western blot, CC reactivity, and
260 immunohistochemistry results were analyzed by one- or two-way ANOVA and followed by Tukey
261 post-test according to each analysis. The in vivo results were analyzed by repeated-measures two-
262 way ANOVA and followed by Tukey post-test. The models' assumptions were investigated by
263 inspecting Q-Q plots and data were logarithmically transformed when necessary to generate a
264 Gaussian-distributed data set. Relaxation responses were expressed as the percentage change from
265 pre-contraction induced by phenylephrine. Concentration-effect curves were submitted to
266 nonlinear regression analysis using the GraphPad Prism program (GraphPad Prism 9.0; GraphPad
267 Software Inc., San Diego, CA, USA). Relaxant potency and maximal response were expressed as

268 pEC50 (negative logarithm of molar concentration producing 50% of the maximal response) and
269 Emax (maximal effect produced by the agonist), respectively. Statistical analysis of the Emax and
270 pEC50 values was performed using nonlinear regression followed by Student's t-test or one-way
271 ANOVA. Values of p less than 0.05 were considered statistically significant.

272

273 **3. Results**

274 **Effect of endothelin-1 receptor inhibition on erectile function and NLRP3 inflammasome**
275 **activity in DOCA/salt model of hypertension**

276 In vivo cavernosal nerve stimulation in mice induced a frequency-dependent increase of ICP
277 (figure 1b and 1c). When mice were treated with the vehicle (for bosentan), ICP/MAP was reduced
278 in Deoxycorticosterone acetate (DOCA)/salt mice at the frequencies from 4 to 20 Hz when
279 compared with unilateral nephrectomized (UNI) mice (Figure 1c). Additionally, DOCA/salt mice
280 had a gradual increment of the blood pressure from day 6 to 9, but then, it was kept sustainedly
281 increased until day 21 (Figure 1d). Bosentan, a non-selective endothelin-1 (ET-1) receptor
282 antagonist, treatment restored the ICP/MAP (Figure 1c) and systolic blood pressure (Figure 1d) in
283 DOCA/salt mice.

284 In the mouse DOCA/salt model of arterial hypertension, there was a trend of increased
285 caspase-1 activity (measured by the caspase-1/pro-caspase-1 ratio) in CC (Figure 1e). IL-1β
286 activity (obtained by the IL-1β/pro-IL-1β) was increased in the CC from DOCA/salt mice (Figure
287 1f). On the other hand, $K_{Ca}2.3$ expression was reduced in DOCA/salt mice CC. Additionally,
288 bosentan prevented the caspase-1 activity trend, IL-1β activity increment, and $K_{Ca}2.3$ expression

289 reduction in CC from DOCA/salt mice (Figure 1e, 1f, and 1g). Moreover, Bosentan also prevented
290 the reduction in the pro-IL-1β in the CC of DOCA/salt mice (Figure 1g). No significant alterations
291 were observed in the expression of pro-caspase-1, caspase-1, and IL-1β (Figure S2a and S2b).

292 DOCA/salt intervention did not modify the contractility to phenylephrine or the relaxation in
293 response to electrical field stimulation of CC (Figure 2b & 2c). Bosentan did not change
294 phenylephrine-induced contraction or the electrical field stimulation-induced relaxation of CC (2d
295 & 2e, Table 1). However, DOCA/salt reduced endothelium-dependent and endothelium-
296 independent relaxations to ACh and SNP, respectively, shifting the concentration-response curves
297 to the right (Figure 2d & 2e, Table 1). Bosentan treatment of DOCA/salt mice prevented these
298 impairments (2d & 2e, Table 1).

299

300 **Effect of NLRP3 inhibition on caspase-1 and IL-1β activity in DOCA/salt mice CC**

301 In the mouse DOCA/salt model of arterial hypertension, there was an increased caspase-1 and
302 IL-1β activity in the CC (Figure S1b). On the other hand, $K_{Ca}2.3$ expression was reduced in
303 DOCA/salt mice CC. Additionally, MCC950 (NLRP3 inhibitor) prevented the caspase-1 and IL-
304 1β activity increment, and $K_{Ca}2.3$ expression reduction in CC from DOCA/salt mice (Figure S1a,
305 S1b and S1c). Furthermore, MCC950 also prevented the reduction in the pro-caspase-1 and pro-
306 IL-1β in the CC of DOCA/salt mice (Figure S2c, S2d). No significant alterations were observed
307 in the expression of caspase-1 and IL-1β (Figure S2c, S2d).

308

309 **ET-1 inhibited the KCa2.2/2.3 channels in endothelial cells, impaired the erectile function**
310 **and activated the NLRP3.**

311 The activity of KCa2.2/2.3 channels using whole cell voltage clamp was measured. The K^+
312 currents were measured in response to a voltage-step protocol. The total membrane conductance
313 was significantly suppressed in the presence of ET-1 (Figure 3c). The activity of NLRP3 in
314 endothelial cells was evaluated by Western blot for caspase-1 (Figure 3d) and IL-1β activity
315 (Figure 3e), or K_{Ca}2.3 expression. These Western blot results suggest that ET-1 administration
316 increased the NLRP3 activity and reduced the KCa.2.3 expression.

317 The incubation of CC endothelial cells with NS13001, a KCa2.2/2.3 opener, or MCC950
318 (NLRP3 inhibitor) significantly reversed the ET-1-induced reduction of the background membrane
319 conductance (Figure 3c) and reduced the NLRP3 activity (Figure 3d & 3e) and increased K_{Ca}2.3
320 (Figure 3f). Additionally, the incubation with apamin, a K_{Ca}2.2/2.3 blocker, did not alter blockage
321 to the total membrane conductance (Figure 3c) and the NLRP3 activity (Figure 3d & 3e) or K_{Ca}2.3
322 expression (Figure 3f) promoted by ET-1 in endothelial cells from murine CC.

323 Intracavernosal administration of NS13001 rescued ET-1's reduction in the ICP/MAP
324 responses to submaximal stimuli at 45, 55, and 65 min. Additionally, apamin did not affect ET-1's
325 impairment of ICP/MAP after its administration (Figure S2b). ET-1 did not change the ICP/MAP
326 responses evoked by maximal stimuli (Figure S2a). Additionally, NS13001 rescued ET-1's
327 reduction in the ICP/MAP responses to maximal stimuli (Figure S2c).

328

329 **Effect of K_{Ca}2.2/2.3 opener on ET1-induced erectile dysfunction and NLRP3 activity in**
330 **DOCA/salt model of hypertension**

331 A selective K_{Ca}2.2/2.3 opener NS13001 restored erectile function (Figure 4c) and normalized
332 systolic blood pressure (Figure 4d) in DOCA/salt-treated mice. NS13001 also prevented the
333 increment in the caspase-1 and IL-1β activity in the CC from DOCA/salt mice (Figure 4e and 4f).
334 Additionally, NS13001 prevented the reduction in the K_{Ca}2.3 expression (Figure 4g). Moreover,
335 pro-IL-1β expression reduction in the CC from DOCA/salt mice was prevented by NS13001
336 treatment (Figure S4b). NS13001 impaired electric-field-stimulation-induced relaxation at 2 and
337 4 Hz (Figure 5c). NS13001 prevented the impaired CC relaxation to ACh and SNP promoted by
338 DOCA/salt (Figure 5d & 5e, Table 1).

339

340 **The K_{Ca}2.2/2.3 blocker apamin did not affect the ET1-induced erectile dysfunction and**
341 **NLRP3 activity in DOCA/salt model of hypertension**

342 A selective K_{Ca}2.2/2.3 blocker, apamin, impaired erectile function (Figure 6c) and elevated
343 the systolic blood pressure in UNI mice (Figure 6d). Curiously, apamin treatment restored erectile
344 function (Figure 6c) and normalized systolic blood pressure (Figure 6d) in DOCA/salt mice.
345 Apamin also prevented caspase-1 and IL-1β increment in the CC from DOCA/salt mice (Figure
346 6e and f). Pro-caspase-1 expression was reduced by apamin treatment in the CC of DOCA/salt
347 mice (Figure S4c & S4d). Furthermore, apamin prevented K_{Ca}2.3 expression reduction in the CC
348 of DOCA/salt mice (Figure 6g). Apamin impaired electric-field-stimulation-induced relaxation at
349 the frequencies 8, 16 and 20 Hz (Figure 7b, Table 1). Apamin also prevented the impaired
350 relaxation to ACh and SNP promoted by DOCA/salt treatment (Figure 7c & 7d, Table 1).

351 **4. Discussion**

352 In this study, we found KCa 2.3 channels play a pivotal role in counteracting ET-1-induced
353 NLRP3 activation and subsequent impairment in vascular and erectile function in DOCA/salt
354 hypertensive mice. This study shows that NS13001, a $K_{Ca}2.3/K_{Ca}2.2$ channel opener, has
355 therapeutic potential by inhibiting the ET-1 and NLRP3 inflammatory pathways and restoring
356 erectile function. It has been shown that NS13001 has a higher affinity for $K_{Ca}2.3$, and there is no
357 strong evidence for $K_{Ca}2.2$ modulation on endothelial and erectile dysfunction[2,25]. The increase
358 in $K_{Ca}2.3$ expression in hypertensive mice highlights its relevance in hypertension. Furthermore,
359 as the ET-1 receptor antagonist, bosentan, normalized blood pressure and erectile function in
360 DOCA/salt mice, it underscores the central role of ET-1 in these dysfunctions, and we suggest that
361 it is modulated through the potassium channels.

362 In the previous study, we showed that NLRP3 modulates erectile function in mice[4]. In
363 addition, it was shown that ET-1-induced erectile dysfunction and pro-inflammatory effect
364 depends on NLRP3 activation[26]. These findings offer valuable insights into the intricate
365 interplay among ET-1, $K_{Ca}2.2/2.3$ channels, and NLRP3 inflammasome, suggesting potential
366 targets for novel therapeutic interventions for inflammatory-related diseases and the restoration of
367 erectile function.

368 In accordance with our study, several previous studies reported that DOCA/salt treatment
369 leads to hypertension in rodents [7,8,27]. We found that the DOCA/salt mouse model presented a
370 gradual increase in blood pressure, impairment in erectile function, and reduced relaxation to ACh
371 and SNP, i.e., endothelium-dependent and endothelium-independent relaxations,
372 respectively[1,21]. The detrimental effect of DOCA/salt hypertension in rodents on erectile

373 dysfunction was reported previously [21,28]. However, the mechanism behind it was not
374 elucidated. We found in this study that it is associated with ET-1 signaling, leading to changes in
375 the expression of K_{Ca}2.3 and the NLRP3 inflammasome.

376 ET-1 treatment leads to endothelial dysfunction, mainly by reducing the function of various
377 populations of potassium channels, such as inward rectifier (Kir)[28], sensitive ATP
378 (KATP)[29,30], voltage-gated (Kv)[31], and calcium-activated (KCa) [15] potassium channels.
379 Moreover, it was already shown that ET-1 exposure releases pro-inflammatory cytokines, like
380 TNF-α [29] and e IL-1β, in monocytes [30] and smooth muscle cells [31]. Accordingly, in this
381 study, treatment with bosentan, an ET-1 type A (ET_A) and B (ET_B) receptor antagonist[32], or
382 MCC950, an NLRP3 inhibitor, restored the K_{Ca}2.3 abundance and reduced NLRP3 activity in
383 DOCA/salt mice, suggesting that ET-1 activity in the CC of DOCA/salt mice is mediated via
384 NLRP3 activation[4,26]. Furthermore, treatment with bosentan restored blood pressure, erectile
385 function, and ACh- and SNP-induced relaxation, suggesting that ET-1 signaling contributes to
386 these abnormalities in the DOCA/salt model of hypertension. This is in line with previous reports
387 that administration of ET-1 antagonists reduces the elevation of blood pressure, reverses cardiac
388 hypertrophy and arterial remodeling [16], left ventricular fibrosis [17,18], inflammation, and renal
389 hypertrophy [18].

390 Accordingly, ET-1 reduces the total membrane conductance in endothelial cells, and our
391 interventions with the K_{Ca}2.2/2.3 activator and inhibitor, or NLRP3 inhibitor suggest that this
392 effect is primarily because of the impairment to K_{Ca}2.2/2.3 function and NLRP3 inhibition.
393 Notably, the K_{Ca}2.3 is expressed explicitly in endothelial but not smooth muscle cells of corpus
394 cavernosum[2]. The K_{Ca}2.2 is also expressed in mouse corpus cavernosum, but the role and
395 location of the expression is less known[33] . It has previously been shown that ET-1 leads to

396 endothelial dysfunction in the pulmonary artery, but mainly, this effect was mediated via reduction
397 of the intermediate-conductance calcium-activated potassium channels, i.e., $K_{Ca}3.1$[15]. ET-1 was
398 also shown to inhibit the $K_{Ca}1.1$ in cultured smooth muscle cells from porcine coronary artery [34].
399 Therefore, this is the first time the inhibitory effect of ET-1 on $K_{Ca}2.3/2.2$ activity has been
400 reported in endothelial cells.

401 Administration of the $K_{Ca}2.2/2.3$ modulator, NS13001, or MCC950, restored the $K_{Ca}2.2/2.3$
402 current in endothelial cells incubated with ET-1. Interestingly, it also reduced the NLRP3 activity
403 and restored both endothelium-dependent and endothelium-independent relaxations impaired by
404 exposure to ET-1. $K_{Ca}2.3$ channels were suggested to be involved in endothelium-dependent
405 vasodilatation in human and rat intracavernous penile arteries [12,13]. $K_{Ca}2.3$ activation regulates
406 l-arginine uptake through the y+ transporter system and increased NO release[5], which will
407 counteract the effect of ET-1.

408 The treatment with NS13001 also reduced caspase-1 and pro-IL-β activity and restored $K_{Ca}2.3$
409 abundance in DOCA/salt mice CC. It can also be mediated via an anti-inflammatory effect of the
410 $K_{Ca}2.2/2.3$ channels, mainly, because it is known to inhibit the release of proinflammatory
411 cytokines such as IL-6, TNF-α, and the migration of immune system cells[35]. Interestingly, the
412 treatment with apamin reduced $K_{Ca}2.3$ expression in the CC of unilaterally nephrectomized mice
413 with no effect in DOCA/salt hypertensive mice, possibly because it is already downregulated.
414 Following our suggestion about the anti-inflammatory effect of the $K_{Ca}2.3$, apamin administration
415 increased caspase-1 and IL-β activity in DOCA/salt mice CC but not in UNI. Here, it is possible
416 to suggest that the reduction in the $K_{Ca}2.3$ expression correlates with the impairment of its function,
417 once the apamin treatment reduces the $K_{Ca}2.3$ expression. Additionally, apamin has a pro-
418 inflammatory action [36]. Curiously, apamin lowered blood pressure and increased erectile

419 function in DOCA/salt mice. Apamin has been previously shown to protect against atherosclerosis
420 by reducing lesion burden, lipid levels, inflammation, and fibrotic markers[37]. Furthermore,
421 modulating apamin-sensitive SK (small-conductance Ca^{2+}-activated K^+) current, which influences
422 action potential duration and arrhythmia in failing ventricles, selectively reduces nNOS after-
423 hyperpolarization, and its effects on SK channels can be modified by nNOS inhibition [38-40].
424 Indeed, we observed that apamin increased the CC response to non-adrenergic and non-cholinergic
425 stimulation, suggesting that apamin may be reducing the after-hyperpolarization of the cavernosal
426 nerve.

427 Importantly, the MCC950, a specific NLRP3 inhibitor, restores a mix of $K_{Ca}2.3$ and other
428 ionic currents. In fact, several Ca^{2+}-channels [transient related canonic (TRC) or potential (TRP)
429 channels] or H^+-channels could also lead to K^+ efflux from the cell, and this mechanism could be
430 responsible for NLRP3 activation [19]. Then, the MCC950 mechanism of NLRP3 inhibition could
431 be related to the modulation of these channels. Additionally, an administration of MCC950
432 prevented the erectile dysfunction induced by ET-1. Previous data from our lab had already shown
433 that the NLRP3 genetic deletion or pharmacological inhibition prevents the impairment of
434 endothelium-dependent relaxation evoked by ET-1 in mice CC[26]. Indeed, ET-1, via ET receptor
435 A or B increase cytosolic Ca^{2+} concentration in vascular smooth muscle cells [41], liver cells and
436 cardiomyocytes[42,43].

437 *Limitations*

438 Limitations to this study include the possibility of investigating only males. This study focused
439 on the vascular mechanisms of erectile dysfunction, which opens the possibility to study only
440 males. In addition, the ICP/MAP ratio was used to measure the erectile function under isoflurane

441 anesthesia. Isoflurane is known to depress the cardiovascular system not only by direct action but
442 also by suppression of the sympathetic nervous system **[44,45]**. This depression in sympathetic
443 activity is closely linked to the increased blood pressure in DOCA/salt mice. In the present study,
444 we cannot exclude off-target effects of the small molecules used to activate K_{Ca}2.2/2.3 channels
445 and of the endothelin receptor antagonist, bosentan. In previous studies, we examined the effect of
446 global NLRP3 knockdown in mice, as well as the up- and downregulation of K_{Ca}2.3 channels, on
447 erectile function [2,4]. Other genetic approaches allowing tissue-specific knockout and/or genetic
448 manipulation by use of Cas/CRISPR may provide additional information on the effect on the
449 NLRP3 inflammasome by modulation of K_{Ca}2.3 channels [46,47].

450

451 **5. Conclusions**

452 In conclusion, our study shows the role of K_{Ca} 2.3 channels in ET-1-induced NLRP3 activation
453 and subsequent impairment in vascular and erectile function in DOCA/salt hypertensive mice. The
454 novel findings highlight the therapeutic potential of the K_{Ca} 2.2/2.3 channel modulator, NS13001,
455 in inhibiting the ET-1 and NLRP3 inflammatory pathways, ultimately leading to the restoration of
456 erectile function. The observed compensatory increase in the K_{Ca}2.3 expression in hypertensive
457 mice underscores its significance in hypertension. Furthermore, the efficacy of the ET-1 receptor
458 antagonist, bosentan, in attenuating these effects emphasizes the central role of ET-1 in inducing
459 vascular and erectile dysfunction through the modulation of potassium channels. Our results
460 provide valuable insights into the complex interplay between ET-1, K_{Ca} 2.2/2.3 channels, and
461 NLRP3 inflammatory-related diseases, paving the way for potential therapeutic interventions
462 targeting these pathways to ameliorate inflammatory-related diseases and restore erectile function.

463 **Abbreviations**

464 The following abbreviations are used in this manuscript:

Ca^{2+}	Calcium
K^+	Potassium
K_{Ca} 2.3	Ca2+-activated K+ channels type 2.3
ET-1	endothelin-1
ICP	intracavernous pressure
CC	corpus cavernosum
IL	interleukin
SK_{Ca}	Small conductance Ca^{2+}-activated K^+ channels
IK_{Ca}	Intermediate conductance Ca^{2+}-activated K^+ channels
BK_{Ca}	Large conductance Ca^{2+}-activated K^+ channels
ED	Erectile dysfunction
NO	Nitric oxide
eNOS	Endothelial NO synthase
TNF-α	Tumor necrosis factor-alpha

K_{ir}	Inward-rectifying K^+ channels
K_{ATP}	ATP-sensitive K^+ channels
K_v	Voltage-gated K^+ channels
DOCA	Deoxycorticosterone acetate
UNI	Unilaterally nephrectomized
SBP	Systolic blood pressure
ICAM2	Intracellular adhesion molecule 2
MAP	mean arterial pressure
ACh	Acetylcholine
SNP	Sodium nitroprusside

Acknowledgments: We want to express profound gratitude for the support from the funding grants PHAB Level 3, AHA Postdoctoral fellowship (24POST1243617), the Sao Paulo Research Foundation (FAPESP, 2016/11988-5; 2016/07641-0; 2018/05638-7; 2019/19749-8); Novo Nordisk Foundation (NFF130C0007739; NFF60C0023284) and Wilhelm Pedersen and Wife's memorial grant.

472 **References**

473 1. Carneiro, F.S.; Giachini, F.R.; Lima, V.V.; Carneiro, Z.N.; Nunes, K.P.; Ergul, A.; Leite,
474 R.; Tostes, R.C.; Webb, R.C. DOCA-salt treatment enhances responses to endothelin-1 in
475 murine corpus cavernosum. *Can J Physiol Pharmacol* **2008**, *86*, 320-328,
476 doi:10.1139/Y08-031.

477 2. Comerma-Steffensen, S.; Kun, A.; Hedegaard, E.R.; Mogensen, S.; Aalkjaer, C.; Kohler,
478 R.; Monster Christensen, B.; Simonsen, U. Down-regulation of K(Ca)2.3 channels causes
479 erectile dysfunction in mice. *Sci Rep* **2017**, *7*, 3839, doi:10.1038/s41598-017-04188-5.

480 3. Comerma-Steffensen, S.G.; Carvacho, I.; Hedegaard, E.R.; Simonsen, U. Small and
481 Intermediate Calcium-Activated Potassium Channel Openers Improve Rat Endothelial and
482 Erectile Function. *Front Pharmacol* **2017**, *8*, 660, doi:10.3389/fphar.2017.00660.

483 4. Fais, R.S.; Rodrigues, F.L.; Pereira, C.A.; Mendes, A.C.; Mestriner, F.; Tostes, R.C.;
484 Carneiro, F.S. The inflammasome NLRP3 plays a dual role on mouse corpora cavernosa
485 relaxation. *Sci Rep* **2019**, *9*, 16224, doi:10.1038/s41598-019-52831-0.

486 5. Simonsen, U.; Winther, A.K.; Olivan-Viguera, A.; Comerma-Steffensen, S.; Kohler, R.;
487 Bek, T. Extracellular l-arginine Enhances Relaxations Induced by Opening of Calcium-
488 Activated SKCa Channels in Porcine Retinal Arteriole. *Int J Mol Sci* **2019**, *20*,
489 doi:10.3390/ijms20082032.

490 6. Kloza, M.; Baranowska-Kuczko, M.; Malinowska, B.; Karpinska, O.; Harasim-Symbor,
491 E.; Kasacka, I.; Kozlowska, H. The influence of DOCA-salt hypertension and chronic
492 administration of the FAAH inhibitor URB597 on K(Ca)2.3/K(Ca)3.1-EDH-type
493 relaxation in rat small mesenteric arteries. *Vascul Pharmacol* **2017**, *99*, 65-73,
494 doi:10.1016/j.vph.2017.10.001.

495 7. Fhaner, M.J.; Galligan, J.J.; Swain, G.M. Increased catecholamine secretion from single
496 adrenal chromaffin cells in DOCA-salt hypertension is associated with potassium channel
497 dysfunction. *ACS Chem Neurosci* **2013**, *4*, 1404-1413, doi:10.1021/cn400115v.

498 8. Matsumoto, T.; Szasz, T.; Tostes, R.C.; Webb, R.C. Impaired beta-adrenoceptor-induced
499 relaxation in small mesenteric arteries from DOCA-salt hypertensive rats is due to reduced
500 K(Ca) channel activity. *Pharmacol Res* **2012**, *65*, 537-545,
501 doi:10.1016/j.phrs.2012.02.004.

502 9. Alexander, S.P.; Mathie, A.; Peters, J.A. Guide to Receptors and Channels (GRAC), 5th
503 edition. *British journal of pharmacology* **2011**, *164 Suppl 1*, S1-324, doi:10.1111/j.1476-
504 5381.2011.01649_1.x.

505 10. Dong, J.Y.; Zhang, Y.H.; Qin, L.Q. Erectile dysfunction and risk of cardiovascular disease:
506 meta-analysis of prospective cohort studies. *J Am Coll Cardiol* **2011**, *58*, 1378-1385,
507 doi:10.1016/j.jacc.2011.06.024.

508 11. Jackson, G. Erectile dysfunction and cardiovascular disease. *Arab J Urol* **2013**, *11*, 212-
509 216, doi:10.1016/j.aju.2013.03.003.

510 12. Kun, A.; Kiraly, I.; Pataricza, J.; Marton, Z.; Krassoi, I.; Varro, A.; Simonsen, U.; Papp,
511 J.G.; Pajor, L. C-type natriuretic peptide hyperpolarizes and relaxes human penile
512 resistance arteries. *J Sex Med* **2008**, *5*, 1114-1125, doi:10.1111/j.1743-6109.2008.00775.x.

513 13. Schjorring, O.; Kun, A.; Flyvbjerg, A.; Kirkeby, H.J.; Jensen, J.B.; Simonsen, U. Flow-
514 evoked vasodilation is blunted in penile arteries from Zucker diabetic fatty rats. *J Sex Med*
515 **2012**, *9*, 1789-1800, doi:10.1111/j.1743-6109.2012.02743.x.

516 14. Behringer, E.J.; Hakim, M.A. Functional Interaction among K(Ca) and TRP Channels for
517 Cardiovascular Physiology: Modern Perspectives on Aging and Chronic Disease. *Int J Mol*
518 *Sci* **2019**, *20*, doi:10.3390/ijms20061380.

519 15. Peng, W.; Michael, J.R.; Hoidal, J.R.; Karwande, S.V.; Farrukh, I.S. ET-1 modulates KCa-
520 channel activity and arterial tension in normoxic and hypoxic human pulmonary
521 vasculature. *Am J Physiol* **1998**, *275*, L729-739, doi:10.1152/ajplung.1998.275.4.L729.

522 16. Li, J.S.; Lariviere, R.; Schiffrin, E.L. Effect of a nonselective endothelin antagonist on
523 vascular remodeling in deoxycorticosterone acetate-salt hypertensive rats. Evidence for a
524 role of endothelin in vascular hypertrophy. *Hypertension* **1994**, *24*, 183-188,
525 doi:10.1161/01.hyp.24.2.183.

526 17. Ammarguellat, F.; Larouche, I.; Schiffrin, E.L. Myocardial fibrosis in DOCA-salt
527 hypertensive rats: effect of endothelin ET(A) receptor antagonism. *Circulation* **2001**, *103*,
528 319-324, doi:10.1161/01.cir.103.2.319.

529 18. Ammarguellat, F.Z.; Gannon, P.O.; Amiri, F.; Schiffrin, E.L. Fibrosis, matrix
530 metalloproteinases, and inflammation in the heart of DOCA-salt hypertensive rats: role of
531 ET(A) receptors. *Hypertension* **2002**, *39*, 679-684, doi:10.1161/hy0202.103481.

532 19. Hafner-Bratkovic, I.; Pelegrin, P. Ion homeostasis and ion channels in NLRP3
533 inflammasome activation and regulation. *Curr Opin Immunol* **2018**, *52*, 8-17,
534 doi:10.1016/j.coi.2018.03.010.

535 20. McGrath, J.C.; Lilley, E. Implementing guidelines on reporting research using animals
536 (ARRIVE etc.): new requirements for publication in BJP. *Br J Pharmacol* **2015**, *172*, 3189-
537 3193, doi:10.1111/bph.12955.

538 21. Carneiro, F.S.; Nunes, K.P.; Giachini, F.R.; Lima, V.V.; Carneiro, Z.N.; Nogueira, E.F.;
539 Leite, R.; Ergul, A.; Rainey, W.E.; Clinton Webb, R.; et al. Activation of the ET-1/ETA
540 pathway contributes to erectile dysfunction associated with mineralocorticoid
541 hypertension. *J Sex Med* **2008**, *5*, 2793-2807, doi:10.1111/j.1743-6109.2008.01009.x.

542 22. Gilda, J.E.; Gomes, A.V. Stain-Free total protein staining is a superior loading control to
543 beta-actin for Western blots. *Anal Biochem* **2013**, *440*, 186-188,
544 doi:10.1016/j.ab.2013.05.027.

545 23. Maloy, A.; Alexander, S.; Andreas, A.; Nyunoya, T.; Chandra, D. Stain-Free total-protein
546 normalization enhances the reproducibility of Western blot data. *Anal Biochem* **2022**, *654*,
547 114840, doi:10.1016/j.ab.2022.114840.

548 24. Gurtler, A.; Kunz, N.; Gomolka, M.; Hornhardt, S.; Friedl, A.A.; McDonald, K.; Kohn,
549 J.E.; Posch, A. Stain-Free technology as a normalization tool in Western blot analysis. *Anal*
550 *Biochem* **2013**, *433*, 105-111, doi:10.1016/j.ab.2012.10.010.

551 25. Kasumu, A.W.; Hougaard, C.; Rode, F.; Jacobsen, T.A.; Sabatier, J.M.; Eriksen, B.L.;
552 Strobaek, D.; Liang, X.; Egorova, P.; Vorontsova, D.; et al. Selective positive modulator
553 of calcium-activated potassium channels exerts beneficial effects in a mouse model of
554 spinocerebellar ataxia type 2. *Chem Biol* **2012**, *19*, 1340-1353,
555 doi:10.1016/j.chembiol.2012.07.013.

556 26. Sobrano Fais, R.; Menezes da Costa, R.; Carvalho Mendes, A.; Mestriner, F.; Comerma-
557 Steffensen, S.G.; Tostes, R.C.; Simonsen, U.; Silva Carneiro, F. NLRP3 activation
558 contributes to endothelin-1-induced erectile dysfunction. *J Cell Mol Med* **2023**, *27*, 1-14,
559 doi:10.1111/jcmm.17463.

560 27. Kloza, M.; Baranowska-Kuczko, M.; Malinowska, B.; Karpinska, O.; Harasim-Symbor,
561 E.; Kasacka, I.; Kozlowska, H. The influence of DOCA-salt hypertension and chronic
562 administration of the FAAH inhibitor URB597 on KCa2.3/KCa3.1-EDH-type relaxation
563 in rat small mesenteric arteries. *Vascular pharmacology* **2017**, *99*, 65-73,
564 doi:10.1016/j.vph.2017.10.001.

565 28. Jin, L.; Lagoda, G.; Leite, R.; Webb, R.C.; Burnett, A.L. NADPH oxidase activation: a
566 mechanism of hypertension-associated erectile dysfunction. *The journal of sexual medicine*
567 **2008**, *5*, 544-551, doi:10.1111/j.1743-6109.2007.00733.x.

568 29. Browatzki, M.; Schmidt, J.; Kubler, W.; Kranzhofer, R. Endothelin-1 induces interleukin-
569 6 release via activation of the transcription factor NF-kappaB in human vascular smooth
570 muscle cells. *Basic research in cardiology* **2000**, *95*, 98-105.

571 30. Helset, E.; Sildnes, T.; Seljelid, R.; Konopski, Z.S. Endothelin-1 stimulates human
572 monocytes in vitro to release TNF-alpha , IL-1beta and IL-6. *Mediators of inflammation*
573 **1993**, *2*, 417-422, doi:10.1155/S0962935193000596.

574 31. Kowalczyk, A.; Kleniewska, P.; Kolodziejczyk, M.; Skibska, B.; Goraca, A. The role of
575 endothelin-1 and endothelin receptor antagonists in inflammatory response and sepsis.
576 *Arch Immunol Ther Exp (Warsz)* **2015**, *63*, 41-52, doi:10.1007/s00005-014-0310-1.

577 32. Opitz, C.F.; Ewert, R.; Kirch, W.; Pittrow, D. Inhibition of endothelin receptors in the
578 treatment of pulmonary arterial hypertension: does selectivity matter? *Eur Heart J* **2008**,
579 *29*, 1936-1948, doi:10.1093/eurheartj/ehn234.

580 33. Comerma-Steffensen, S.; Prat-Duran, J.; Mogensen, S.; Fais, R.; Pinilla, E.; Simonsen, U.
581 Erectile Dysfunction and Altered Contribution of KCa1.1 and KCa2.3 Channels in the

582 Penile Tissue of Type-2 Diabetic db/db Mice. *J Sex Med* **2022**, *19*, 697-710,
583 doi:10.1016/j.jsxm.2022.02.021.

584 34. Minami, K.; Hirata, Y.; Tokumura, A.; Nakaya, Y.; Fukuzawa, K. Protein kinase C-
585 independent inhibition of the Ca(2+)-activated K+ channel by angiotensin II and
586 endothelin-1. *Biochemical pharmacology* **1995**, *49*, 1051-1056, doi:10.1016/0006-
587 2952(95)98500-9.

588 35. Dolga, A.M.; Letsche, T.; Gold, M.; Doti, N.; Bacher, M.; Chiamvimonvat, N.; Dodel, R.;
589 Culmsee, C. Activation of KCNN3/SK3/K(Ca)2.3 channels attenuates enhanced calcium
590 influx and inflammatory cytokine production in activated microglia. *Glia* **2012**, *60*, 2050-
591 2064, doi:10.1002/glia.22419.

592 36. Sobral, F.; Sampaio, A.; Falcao, S.; Queiroz, M.J.; Calhelha, R.C.; Vilas-Boas, M.;
593 Ferreira, I.C. Chemical characterization, antioxidant, anti-inflammatory and cytotoxic
594 properties of bee venom collected in Northeast Portugal. *Food and chemical toxicology :*
595 *an international journal published for the British Industrial Biological Research*
596 *Association* **2016**, *94*, 172-177, doi:10.1016/j.fct.2016.06.008.

597 37. Kim, S.J.; Park, J.H.; Kim, K.H.; Lee, W.R.; Pak, S.C.; Han, S.M.; Park, K.K. The
598 Protective Effect of Apamin on LPS/Fat-Induced Atherosclerotic Mice. *Evid Based*
599 *Complement Alternat Med* **2012**, *2012*, 305454, doi:10.1155/2012/305454.

600 38. Koya, T.; Watanabe, M.; Natsui, H.; Kadosaka, T.; Koizumi, T.; Nakao, M.; Hagiwara, H.;
601 Kamada, R.; Temma, T.; Anzai, T. Pharmacological nNOS inhibition modified small-
602 conductance Ca(2+)-activated K(+) channel without altering Ca(2+) dynamics. *Am J*
603 *Physiol Heart Circ Physiol* **2022**, *323*, H869-H878, doi:10.1152/ajpheart.00252.2022.

604 39. Selemidis, S.; Ziogas, J.; Cocks, T.M. Apamin- and nitric oxide-sensitive biphasic non-
605 adrenergic non-cholinergic inhibitory junction potentials in the rat anococcygeus muscle.
606 *J Physiol* **1998**, *513 (Pt 3)*, 835-844, doi:10.1111/j.1469-7793.1998.835ba.x.

607 40. Shuba, M.F.; Vladimirova, I.A. Effect of apamin on the electrical responses of smooth
608 muscle to adenosine 5'-triphosphate and to non-adrenergic, non-cholinergic nerve
609 stimulation. *Neuroscience* **1980**, *5*, 853-859, doi:10.1016/0306-4522(80)90154-2.

610 41. Kawanabe, Y.; Nauli, S.M. Involvement of extracellular Ca2+ influx through voltage-
611 independent Ca2+ channels in endothelin-1 function. *Cellular signalling* **2005**, *17*, 911-
612 916, doi:10.1016/j.cellsig.2005.01.001.

613 42. Jouneaux, C.; Mallat, A.; Serradeil-Le Gal, C.; Goldsmith, P.; Hanoune, J.; Lotersztajn, S.
614 Coupling of endothelin B receptors to the calcium pump and phospholipase C via Gs and
615 Gq in rat liver. *The Journal of biological chemistry* **1994**, *269*, 1845-1851.

616 43. Zeng, Q.; Li, X.; Zhong, G.; Zhang, W.; Sun, C. Endothelin-1 induces intracellular [Ca2+]
617 increase via Ca 2+ influx through the L-type Ca2+ channel, Ca 2+ -induced Ca2+ release
618 and a pathway involving ET A receptors, PKC, PKA and AT1 receptors in cardiomyocytes.
619 *Sci China C Life Sci* **2009**, *52*, 360-370, doi:10.1007/s11427-009-0046-z.

620 44. Seagard, J.L.; Hopp, F.A.; Bosnjak, Z.J.; Osborn, J.L.; Kampine, J.P. Sympathetic efferent
621 nerve activity in conscious and isoflurane-anesthetized dogs. *Anesthesiology* **1984**, *61*,
622 266-270, doi:10.1097/00000542-198409000-00006.

623 45. Constantinides, C.; Mean, R.; Janssen, B.J. Effects of isoflurane anesthesia on the
624 cardiovascular function of the C57BL/6 mouse. *ILAR J* **2011**, *52*, e21-31.

625 46. Gurevich, E.V.; Gurevich, V.V. Beyond traditional pharmacology: new tools and
626 approaches. *Br J Pharmacol* **2015**, *172*, 3229-3241, doi:10.1111/bph.13066.

627 47. Mitchison, T.J. Towards a pharmacological genetics. *Chem Biol* **1994**, *1*, 3-6,
628 doi:10.1016/1074-5521(94)90034-5.

629

630

631

632

633

634

635

636

637

638

639

640

641 **Figure Legends:**

642 **Graphic abstract. Overview of the K_{Ca}2.2/2.3 regulation on the ET-1-induced NLRP3**
643 **inflammasome activation in ECs.** NLRP3 inflammasome activation in ECs depends on
644 endothelin receptor B. On activation, NLRP3 recruits and forms a complex with ASC as well as
645 procaspase 1. In the final step, the assembled inflammasome platform cleaves pro-caspase-1, and
646 caspase-1 cleaves pro–IL-1β to activate IL-1β. NS13001 activates K_{Ca}2.2/2.3, which inhibits ET-
647 1-induced NLRP3 activation. Apamin inhibits K_{Ca}2.2/2.3 opening. Bosentan directly inhibits ETB
648 receptors in ECs, preventing the NLRP3 inflammasome activation.

649

650 **Figure 1. The endothelin receptor antagonist bosentan restores erectile function and inhibits**
651 **inflammation in DOCA/salt mice.** (**a**) Experimental design. (**b**) Original tracings showing the
652 intracavernosal pressure (ICP, lower traces) and mean arterial pressure (MAP, upper traces) in
653 response to cavernosal nerve stimulation assessed over a range of frequencies (0.5-20 Hz) in a
654 unilateral nephrectomized (UNI) and a DOCA/salt (DOCA) hypertensive mice treated with vehicle
655 or bosentan. (**c**) Average responses in ICP/MAP and (**d**) systolic blood pressure of UNI and DOCA
656 hypertensive mice. Immunoblot analysis of (**e**) caspase-1, (**f**) IL-1β, and **(g)** K_{Ca}2.3 expression in
657 CC strips of UNI and DOCA hypertensive mice treated with bosentan or vehicle. The arrow
658 indicates when the treatment started (c). Data represent the mean ± SEM values of the groups. *
659 $p<0.05$. n=5-11. The comparison of each value was performed by two-way ANOVA followed by
660 the Holm-Šídák post-test. ICP=intracavernosal pressure; MAP=mean arterial pressure. The entire
661 membranes for pro-caspase-1, caspase-1, pro-IL-1β, IL-1β, and K_{Ca}2.3 western blots are shown in
662 figures S7 and S8.

663

664 **Figure 2. Bosentan restores the impaired endothelium-dependent and -independent**
665 **relaxations in corpus cavernosum of DOCA/salt mice.** (**a**) Experimental design. (**b**)
666 Concentration-response curves for phenylephrine, (**c**) frequency-response curves for electrical-
667 field-stimulation-induced relaxation, and concentration-response curves for (**d**) ACh and (e) SNP
668 in CC strips of DOCA/salt (DOCA) hypertensive and unilaterally nephrectomized (UNI) mice
669 treated with bosentan or vehicle. The values of the graphics represent mean ± SEM. * $p < 0.05$. n
670 = 6-8. The comparison of pEC_{50} and Emax (table 1) and each value was performed by two-way
671 ANOVA followed by the Holm-Šídák post-test.

672 **Figure 3. An opener of $K_{Ca}2.2/2.3$ channels restores the background membrane conductance**
673 **and inhibits inflammation in primary endothelial cells of corpus cavernosum (CC) after**
674 **endothelin-1 treatment.** (**a**) Experimental design. (**b**) Representative traces from the (**c**) Current
675 evoked by the voltage-step protocol from −100 to +100 mV in endothelial cells in the presence of
676 vehicle or ET-1 (100 nM) and the effect of NS13001 (100 nM) or apamim (100 nM)
677 administration**. The representative traces (upper panel) and the average current-voltage**
678 **relations (lower panel).** Immunoblotting (upper panel) and expression (lower panel) for (**d**)
679 caspase-1 and (**e**) IL-1β in murine *CC* after the administration of vehicle or ET-1 alone or
680 combined with NS13001 and apamin. The data is presented as means ± SEM. *$p \leq 0.05$. n = 3-6.
681 Each value was compared by two-way ANOVA followed by the Holm-Šídák post-test. The entire
682 membranes for pro-caspase-1, caspase-1, pro-IL-1β, and IL-1β western blots are shown in Figure
683 S9 and S10.

684

685 **Figure 4. An opener of $K_{Ca}2$ channels, NS13001, restores erectile function and inhibits**
686 **inflammation in DOCA/salt mice.** (**a**) Experimental design. (**b**) Original tracings showing the
687 intracavernosal pressure (ICP, lower traces) and mean arterial pressure (MAP, upper traces) in
688 response to cavernosal nerve stimulation assessed over a range of frequencies (0.5-20 Hz) in
689 unilateral nephrectomized (UNI) and DOCA/salt (DOCA) hypertensive mice treated with vehicle
690 or NS13001. (**c**) Average responses in ICP/MAP and (**d**) systolic blood pressure of UNI and
691 DOCA mice. Analysis of the (**e**) caspase-1, (**f**) IL-1β**, (g)** and $K_{Ca}2.3$ expression in CC strips from
692 DOCA or UNI mice treated with NS13001 or vehicle. Data represent as mean ± SEM values of
693 the groups. * $p<0.05$. n=5-6. The comparison of each value was performed by two-way ANOVA
694 followed by the Holm-Šídák post-test. ICP=intracavernosal pressure; MAP=mean arterial
695 pressure. The entire membranes for pro-caspase-1, caspase-1, pro-IL-1β, IL-1β, and $K_{Ca}2.3$
696 western blots are shown in figure S11 and S12.

697

698 **Figure 5. NS13001 restores the impaired endothelium-dependent and -independent**
699 **relaxations in corpus cavernosum of DOCA/salt mice.** (**a**) Experimental design. (**b**)
700 Concentration-response curves for phenylephrine, (**c**) frequency-response curves for electrical-
701 field-stimulation-induced relaxation, and concentration-response curves for (**d**) ACh and (**e**) and
702 SNP in CC strips of DOCA/salt (DOCA) hypertensive and unilaterally nephrectomized (UNI)
703 mice treated with NS13001 or vehicle. The values of the graphics represent as mean ± SEM. * p
704 <0.05. n = 6-8. The comparison of pEC_{50} and Emax (table 1) and each value was performed by
705 two-way ANOVA followed by the Holm-Šídák post-test. Figure 5 (b to e) curves share the same
706 UNI and DOCA vehicles as in Figure 3 (b to e).

707

708 **Figure 6. A blocker of $K_{Ca}2.2/2.3$ channels, apamin, inhibits erectile responses in unilaterally**
709 **nephrectomized control mice and restore responses in DOCA/salt treated mice.** (**a**)
710 Experimental design. (**b**) Original tracings showing the intracavernosal pressure (ICP, lower
711 traces) and mean arterial pressure (MAP, upper traces) in response to cavernosal nerve stimulation
712 assessed over a range of frequencies (0.5-20 Hz) in unilateral nephrectomized (UNI) and
713 DOCA/salt (DOCA) hypertensive mice treated with vehicle or apamin. (**c**) Average responses in
714 ICP/MAP and (**d**) systolic blood pressure of UNI and DOCA hypertensive mice. Analysis of the
715 (e) caspase-1, (**f**) IL-1β, and (**g**) $K_{Ca}2.3$ expression in CC strips of DOCA hypertensive or UNI
716 mice treated with apamin or vehicle. Data represent as mean ± SEM values of the groups. * $p<0.05$.
717 n=5-6. Comparisons of each value were performed using a two-way ANOVA followed by the
718 Holm-Šídák post hoc test. ICP=intracavernosal pressure; MAP=mean arterial pressure. The entire
719 membranes for pro-caspase-1, caspase-1, pro-IL-1β, IL-1β, and $K_{Ca}2.3$ western blots are shown in
720 figure S13 and 14.

721

722 **Figure 7. Apamin inhibits relaxation in corpus cavernosum (CC) of unilaterally**
723 **nephrectomized control mice and has no effect on responses in DOCA/salt mice.** (**a**)
724 Experimental design. (**b**) Concentration-response curves for phenylephrine, (**c**) frequency-
725 response curves for electrical-field-stimulation-induced relaxation, and concentration-response
726 curves for (**d**) ACh and (**e**) and SNP in CC strips of DOCA/salt (DOCA) hypertensive and
727 unilaterally nephrectomized (UNI) mice treated with apamin or vehicle. The values of the graphics
728 represent as mean ± SEM. * $p <0.05$. n = 5-6. The comparison of pEC50 and Emax (table 1) and

each value was performed by two-way ANOVA followed by the Holm-Šídák post-test. Figure 8 (a to d) curves share the same UNI and DOCA vehicles as Figure 2 (a to d). Only UNI apamin and DOCA apamin curves were statistically compared.

746 **Table 1. Pharmacological inhibition of ET-1 on DOCA/salt-induced impairment of the CC**
747 **reactivity.** Values of Emax and pEC_{50} for the phenylephrine, ACh, and SNP concentration-effect
748 curves in CC of mice. Curves were performed in CC of unilaterally nephrectomized (UNI) or
749 DOCA/salt-treated mice combined with the treatment with vehicle, bosentan or NS13001.

Pharmacological inhibition of ET-1 on DOCA/salt-induced impairment of the CC reactivity.

Drug	UNI	DOCA/salt	UNI bosentan	DOCA/salt bosentan
phenylephrine				
pEC50	5.89 ± 0.26	5.85 ± 0.30	6.13 ± 0.18	6.04 ± 0.12
Emax (mN)	634 ± 68	689.9 ± 87.56	406.1 ± 29.16	487.4 ± 22.95
ACh				
pEC_{50}	7.05 ± 0.07	6.55 ± 0.11*	7.14 ± 0.07#	7.22 ± 0.06#
Emax(%)	99 ± 3	88 ± 5	97.30 ± 2.80	95.04 ± 2.12
Sodium nitroprusside				
pEC_{50}	7.18 ± 0.05	6.58 ± 0.05*	7.59 ± 0.08#	7.31 ± 0.06#

Emax(%)	100 ± 5	100 ± 3.70	100 ± 2.22	100 ± 3.42

$K_{Ca}2.3$ activity on DOCA/salt-induced impairment in the CC reactivity

Drug	UNI NS13001	DOCA/salt NS13001	**UNI** **apamin**	**DOCA/salt** **apamin**
phenylephrine				
pEC_{50}	6.00 ± 0.14	5.98 ± 0.16	5.877 ± 0.12	6.169 ± 0.17
Emax (mN)	473.6 ± 28.05	434.0 ± 28.99	541.7 ± 27.23	513.6 ± 33.95
ACh				
pEC_{50}	7.16 ± 0.13 #	7.42 ± 0.08#	6.828 ± 0.09	6.795 ± 0.11
Emax(%)	100 ± 5	97.33 ± 3.00	90.90 ± 2.36	89.13 ± 2.76
Sodium nitroprusside				
pEC_{50}	7.00 ±0.06#	7.02 ±0.08#	6.658 ± 0.10*	6.569 ± 0.10*
Emax(%)	100 ± 3	100 ± 3	100 ± 2.21	100 ± 2.40

750 Values are mean ± SEM (n=5-11 in each group). * $p<0.05$ significantly different from unilateral
751 nephrectomized (UNI). # $p<0.05$ significantly different from DOCA/salt (DOCA). The

752 comparison of pEC_{50} and Emax parameters was performed by two-way ANOVA followed by the

753 Holm-Šídák post-test.

754

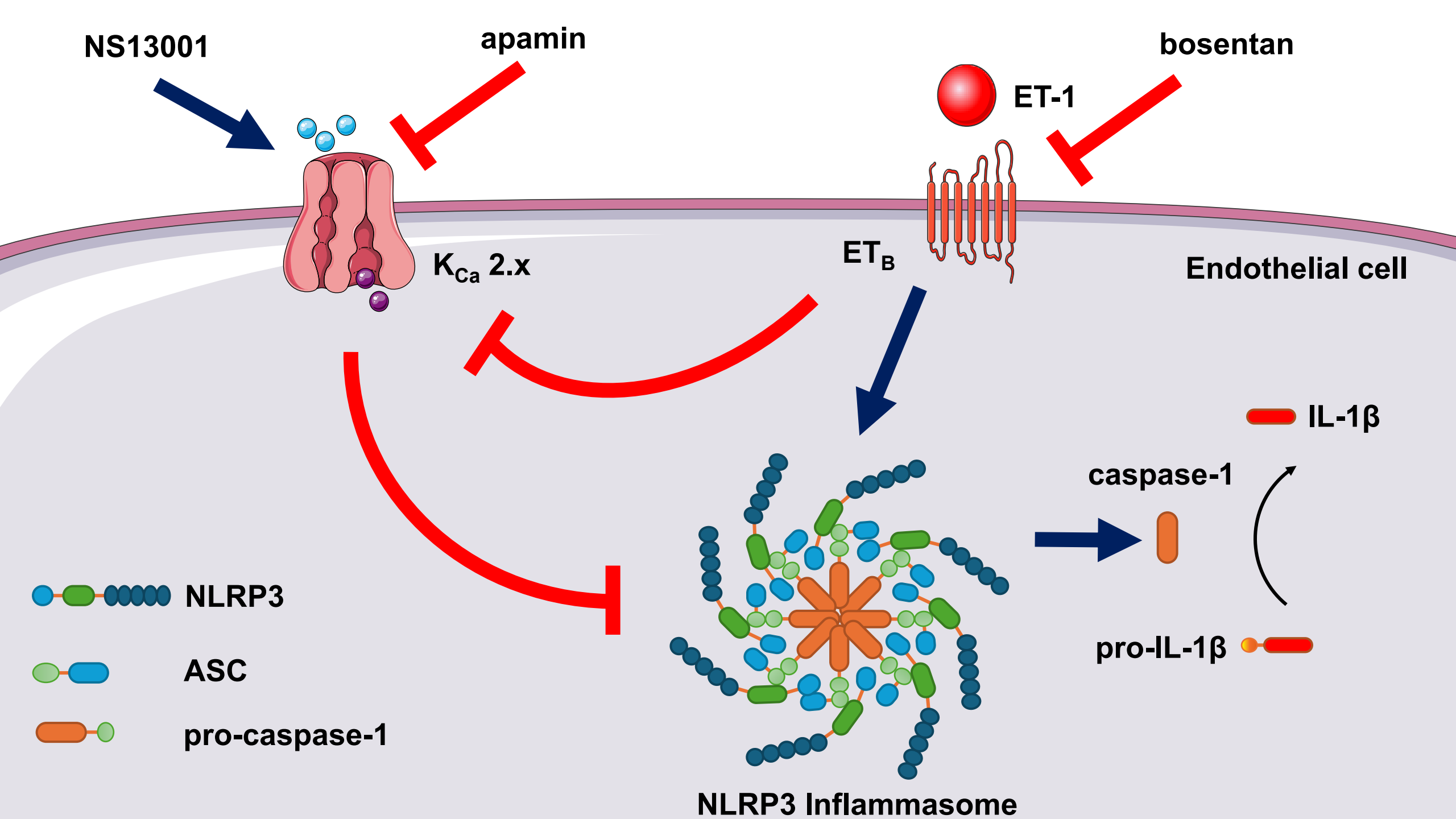
NS13001
apamin
bosentan
ET-1
K_{Ca} 2.x
ET_B
Endothelial cell
IL-1β
caspase-1
pro-IL-1β
NLRP3
ASC
pro-caspase-1
NLRP3 Inflammasome

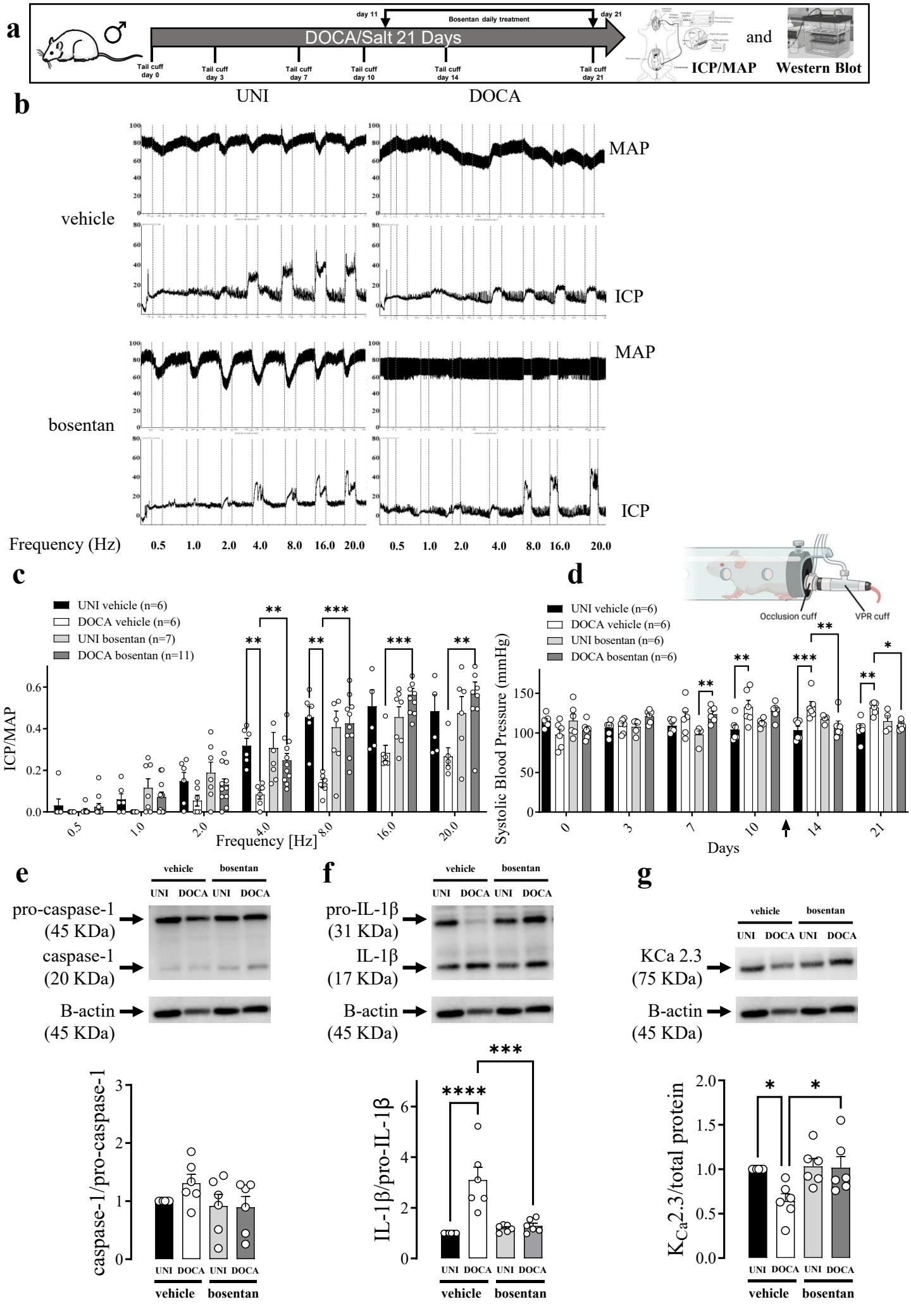
a
day 11
Bosentan daily treatment
day 21
DOCA/Salt 21 Days
Tail cuff day 0
Tail cuff day 3
Tail cuff day 7
Tail cuff day 10
Tail cuff day 14
Tail cuff day 21
ICP/MAP
and
Western Blot
UNI
DOCA
b
vehicle
bosentan
MAP
ICP
Frequency (Hz)
0.5 1.0 2.0 4.0 8.0 16.0 20.0
c
UNI vehicle (n=6)
DOCA vehicle (n=6)
UNI bosentan (n=7)
DOCA bosentan (n=11)
ICP/MAP
Frequency [Hz]
d
Occlusion cuff
VPR cuff
UNI vehicle (n=6)
DOCA vehicle (n=6)
UNI bosentan (n=6)
DOCA bosentan (n=6)
Systolic Blood Pressure (mmHg)
Days
e
vehicle
bosentan
UNI DOCA UNI DOCA
pro-caspase-1 (45 KDa)
caspase-1 (20 KDa)
B-actin (45 KDa)
caspase-1/pro-caspase-1
f
pro-IL-1β (31 KDa)
IL-1β (17 KDa)
B-actin (45 KDa)
IL-1β/pro-IL-1β
g
KCa 2.3 (75 KDa)
B-actin (45 KDa)
KCa2.3/total protein

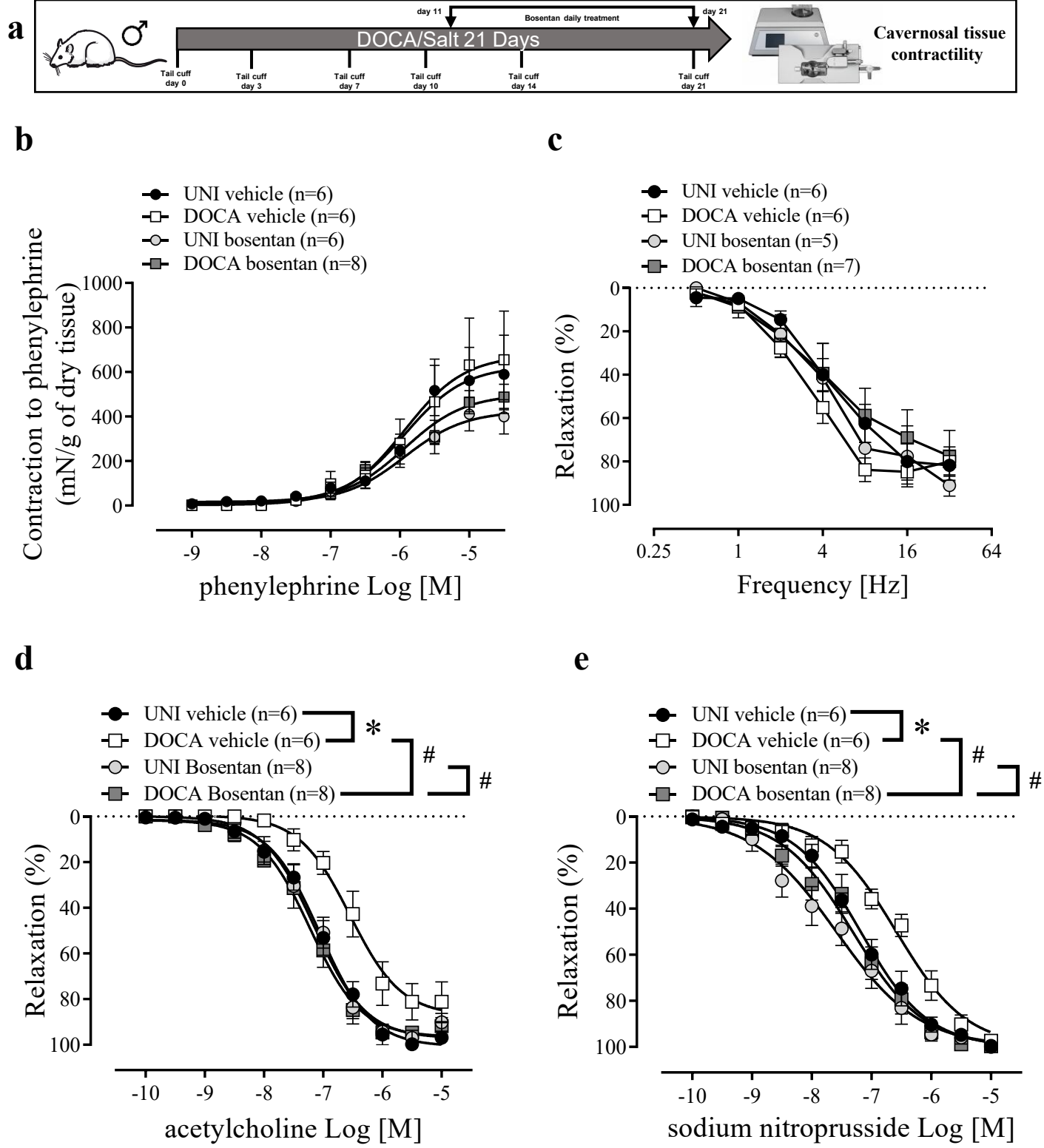
a
day 11
Bosentan daily treatment
day 21
DOCA/Salt 21 Days
Tail cuff day 0
Tail cuff day 3
Tail cuff day 7
Tail cuff day 10
Tail cuff day 14
Tail cuff day 21
Cavernosal tissue contractility
b
UNI vehicle (n=6)
DOCA vehicle (n=6)
UNI bosentan (n=6)
DOCA bosentan (n=8)
Contraction to phenylephrine (mN/g of dry tissue)
phenylephrine Log [M]
c
UNI vehicle (n=6)
DOCA vehicle (n=6)
UNI bosentan (n=5)
DOCA bosentan (n=7)
Relaxation (%)
Frequency [Hz]
d
UNI vehicle (n=6)
DOCA vehicle (n=6)
UNI Bosentan (n=8)
DOCA Bosentan (n=8)
Relaxation (%)
acetylcholine Log [M]
e
UNI vehicle (n=6)
DOCA vehicle (n=6)
UNI bosentan (n=8)
DOCA bosentan (n=8)
Relaxation (%)
sodium nitroprusside Log [M]

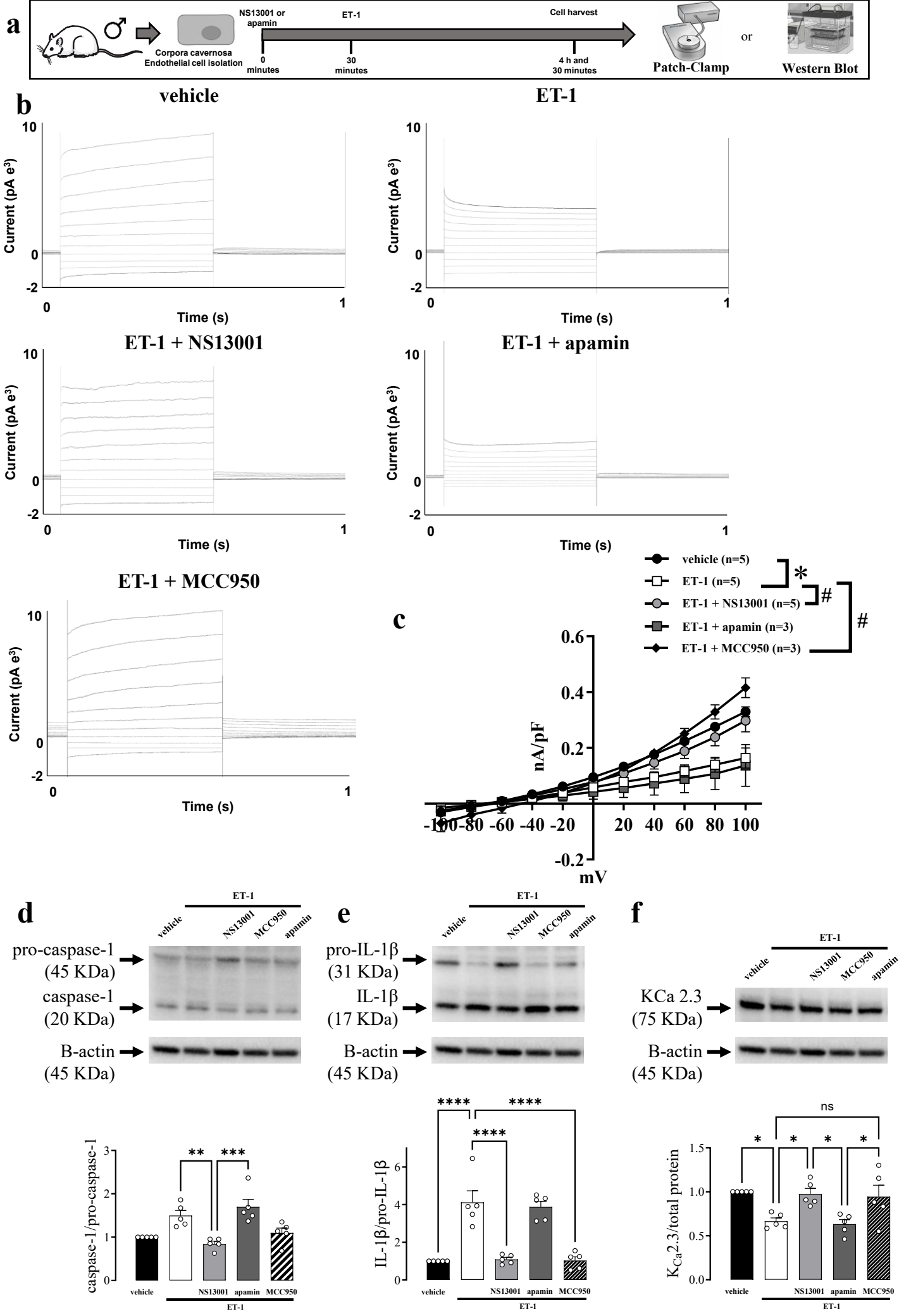
a
Corpora cavernosa
Endothelial cell isolation
NS13001 or apamin
ET-1
Cell harvest
0 minutes
30 minutes
4 h and 30 minutes
Patch-Clamp
or
Western Blot
b
vehicle
ET-1
ET-1 + NS13001
ET-1 + apamin
ET-1 + MCC950
Current (pA e³)
Time (s)
c
vehicle (n=5)
ET-1 (n=5)
ET-1 + NS13001 (n=5)
ET-1 + apamin (n=3)
ET-1 + MCC950 (n=3)
nA/pF
mV
d
ET-1
vehicle
NS13001
MCC950
apamin
pro-caspase-1 (45 KDa)
caspase-1 (20 KDa)
B-actin (45 KDa)
caspase-1/pro-caspase-1
e
pro-IL-1β (31 KDa)
IL-1β (17 KDa)
IL-1β/pro-IL-1β
f
KCa 2.3 (75 KDa)
KCa2.3/total protein
ns

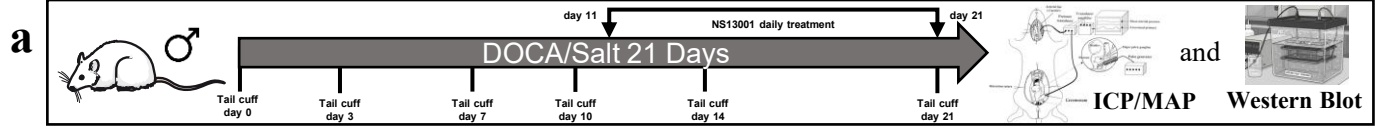
a
day 11
NS13001 daily treatment
day 21
DOCA/Salt 21 Days
Tail cuff day 0
Tail cuff day 3
Tail cuff day 7
Tail cuff day 10
Tail cuff day 14
Tail cuff day 21
and
ICP/MAP
Western Blot

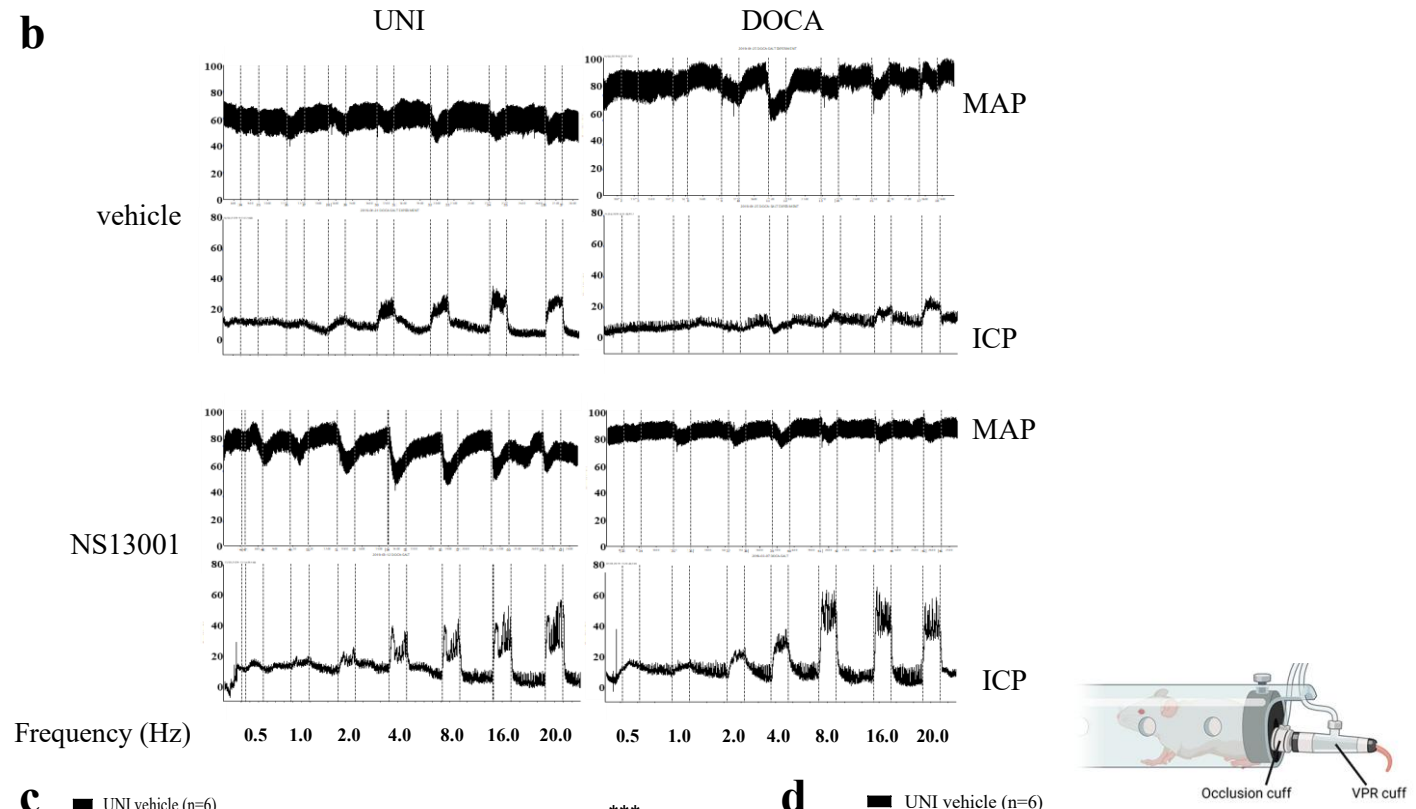
b
UNI
DOCA
vehicle
NS13001
MAP
ICP
Frequency (Hz)
0.5 1.0 2.0 4.0 8.0 16.0 20.0
Occlusion cuff
VPR cuff

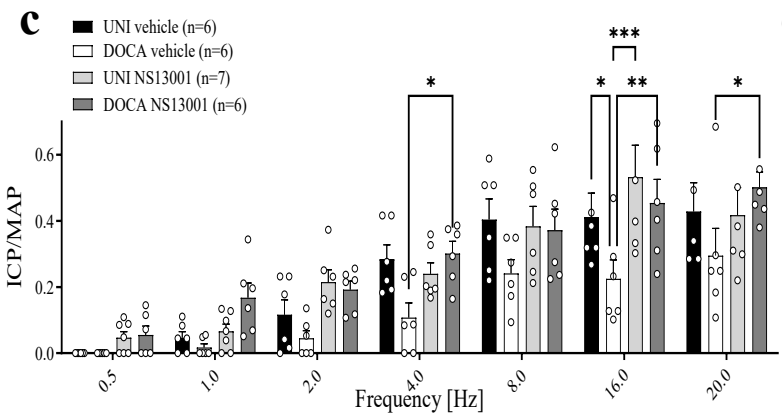
c
UNI vehicle (n=6)
DOCA vehicle (n=6)
UNI NS13001 (n=7)
DOCA NS13001 (n=6)
ICP/MAP
Frequency [Hz]
0.5
1.0
2.0
4.0
8.0
16.0
20.0

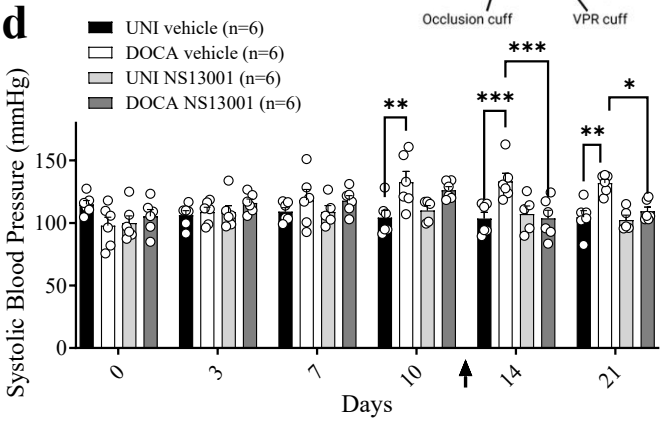
d
UNI vehicle (n=6)
DOCA vehicle (n=6)
UNI NS13001 (n=6)
DOCA NS13001 (n=6)
Systolic Blood Pressure (mmHg)
Days
0
3
7
10
14
21

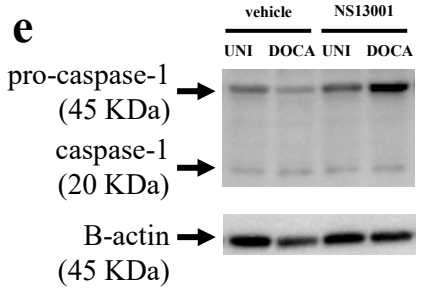
e
vehicle
NS13001
UNI DOCA UNI DOCA
pro-caspase-1
(45 KDa)
caspase-1
(20 KDa)
B-actin
(45 KDa)

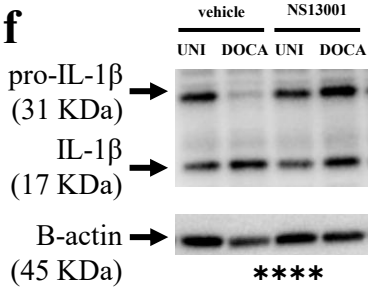
f
vehicle
NS13001
UNI DOCA UNI DOCA
pro-IL-1β
(31 KDa)
IL-1β
(17 KDa)
B-actin
(45 KDa)

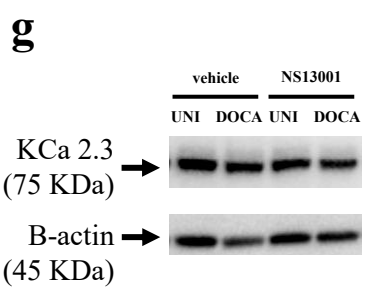
g
vehicle
NS13001
UNI DOCA UNI DOCA
KCa 2.3
(75 KDa)
B-actin
(45 KDa)

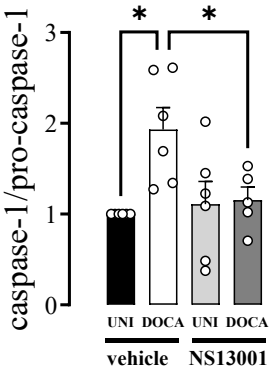
caspase-1/pro-caspase-1
UNI DOCA UNI DOCA
vehicle NS13001

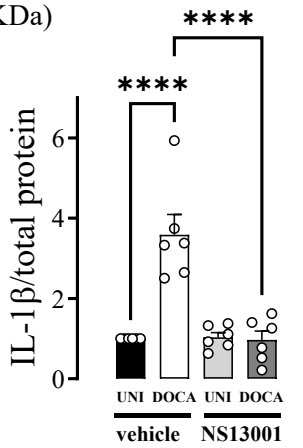
IL-1β/total protein
UNI DOCA UNI DOCA
vehicle NS13001

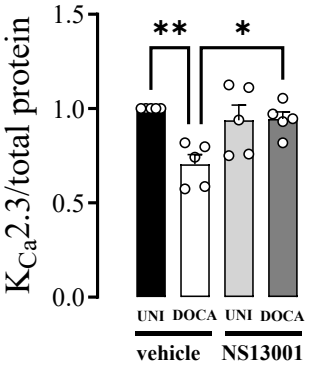
KCa2.3/total protein
UNI DOCA UNI DOCA
vehicle NS13001

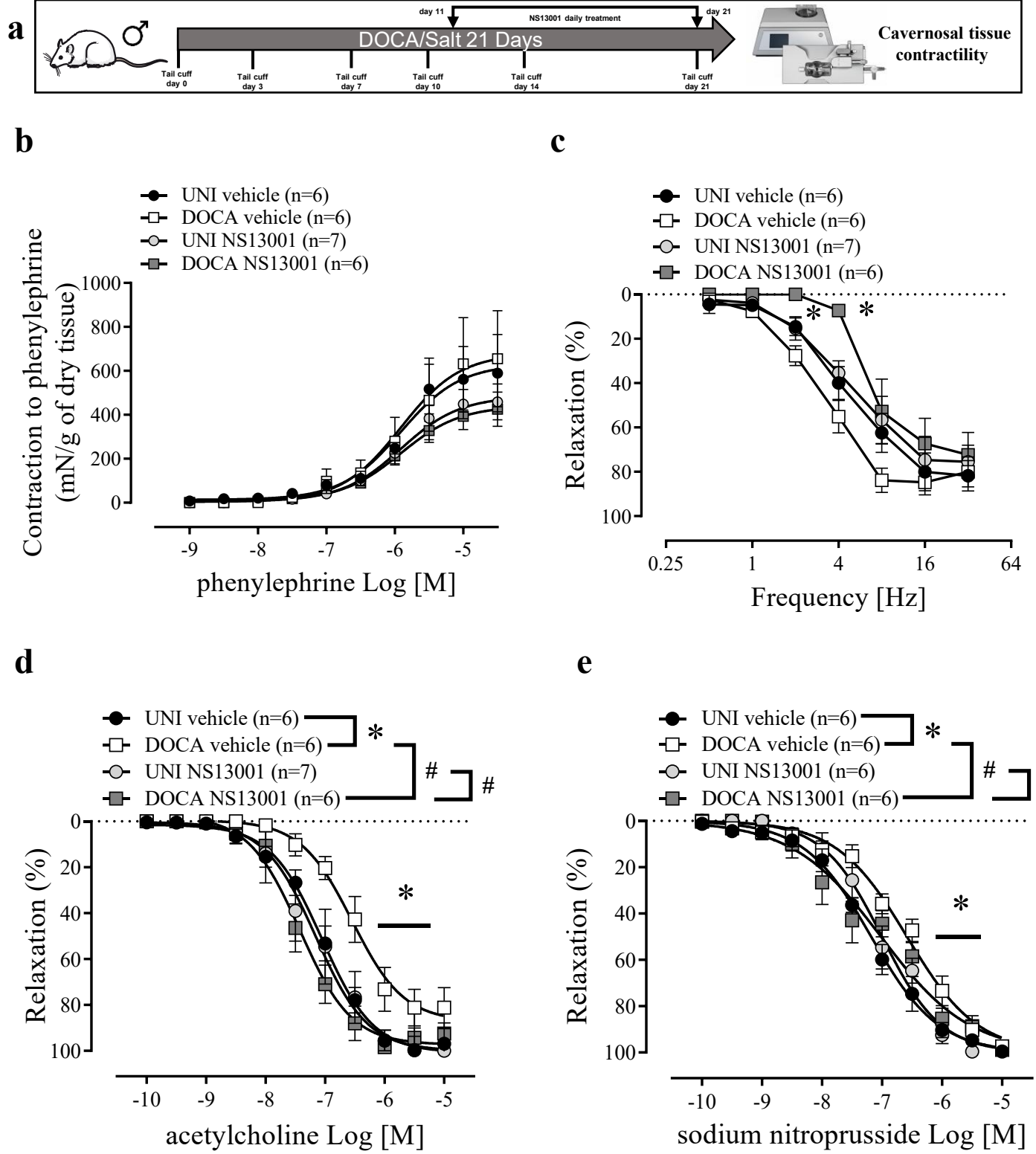
a
day 11
NS13001 daily treatment
day 21
DOCA/Salt 21 Days
Tail cuff day 0
Tail cuff day 3
Tail cuff day 7
Tail cuff day 10
Tail cuff day 14
Tail cuff day 21
Cavernosal tissue contractility
b
UNI vehicle (n=6)
DOCA vehicle (n=6)
UNI NS13001 (n=7)
DOCA NS13001 (n=6)
Contraction to phenylephrine (mN/g of dry tissue)
phenylephrine Log [M]
c
Relaxation (%)
Frequency [Hz]
d
UNI vehicle (n=6)
DOCA vehicle (n=6)
UNI NS13001 (n=7)
DOCA NS13001 (n=6)
Relaxation (%)
acetylcholine Log [M]
e
UNI vehicle (n=6)
DOCA vehicle (n=6)
UNI NS13001 (n=6)
DOCA NS13001 (n=6)
Relaxation (%)
sodium nitroprusside Log [M]

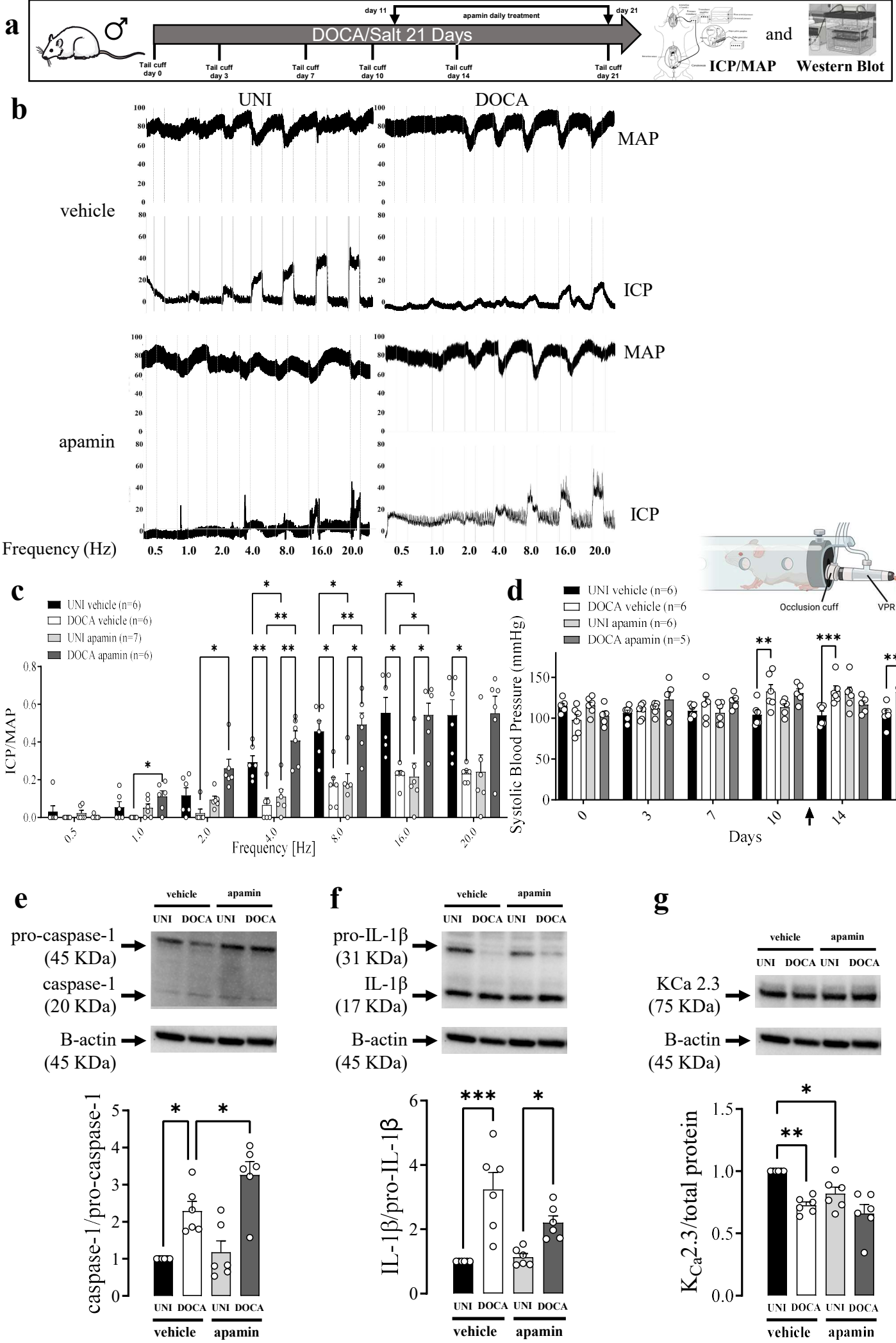
a
DOCA/Salt 21 Days
day 11
day 21
apamin daily treatment
Tail cuff day 0
Tail cuff day 3
Tail cuff day 7
Tail cuff day 10
Tail cuff day 14
Tail cuff day 21
ICP/MAP
and
Western Blot
b
UNI
DOCA
MAP
vehicle
ICP
MAP
apamin
ICP
Frequency (Hz)
0.5 1.0 2.0 4.0 8.0 16.0 20.0
c
UNI vehicle (n=6)
DOCA vehicle (n=6)
UNI apamin (n=7)
DOCA apamin (n=6)
ICP/MAP
Frequency [Hz]
d
UNI vehicle (n=6)
DOCA vehicle (n=6
UNI apamin (n=6)
DOCA apamin (n=5)
Occlusion cuff
VPR cuff
Systolic Blood Pressure (mmHg)
Days
e
vehicle
apamin
UNI DOCA UNI DOCA
pro-caspase-1 (45 KDa)
caspase-1 (20 KDa)
B-actin (45 KDa)
caspase-1/pro-caspase-1
f
pro-IL-1β (31 KDa)
IL-1β (17 KDa)
B-actin (45 KDa)
IL-1β/pro-IL-1β
g
KCa 2.3 (75 KDa)
B-actin (45 KDa)
KCa2.3/total protein

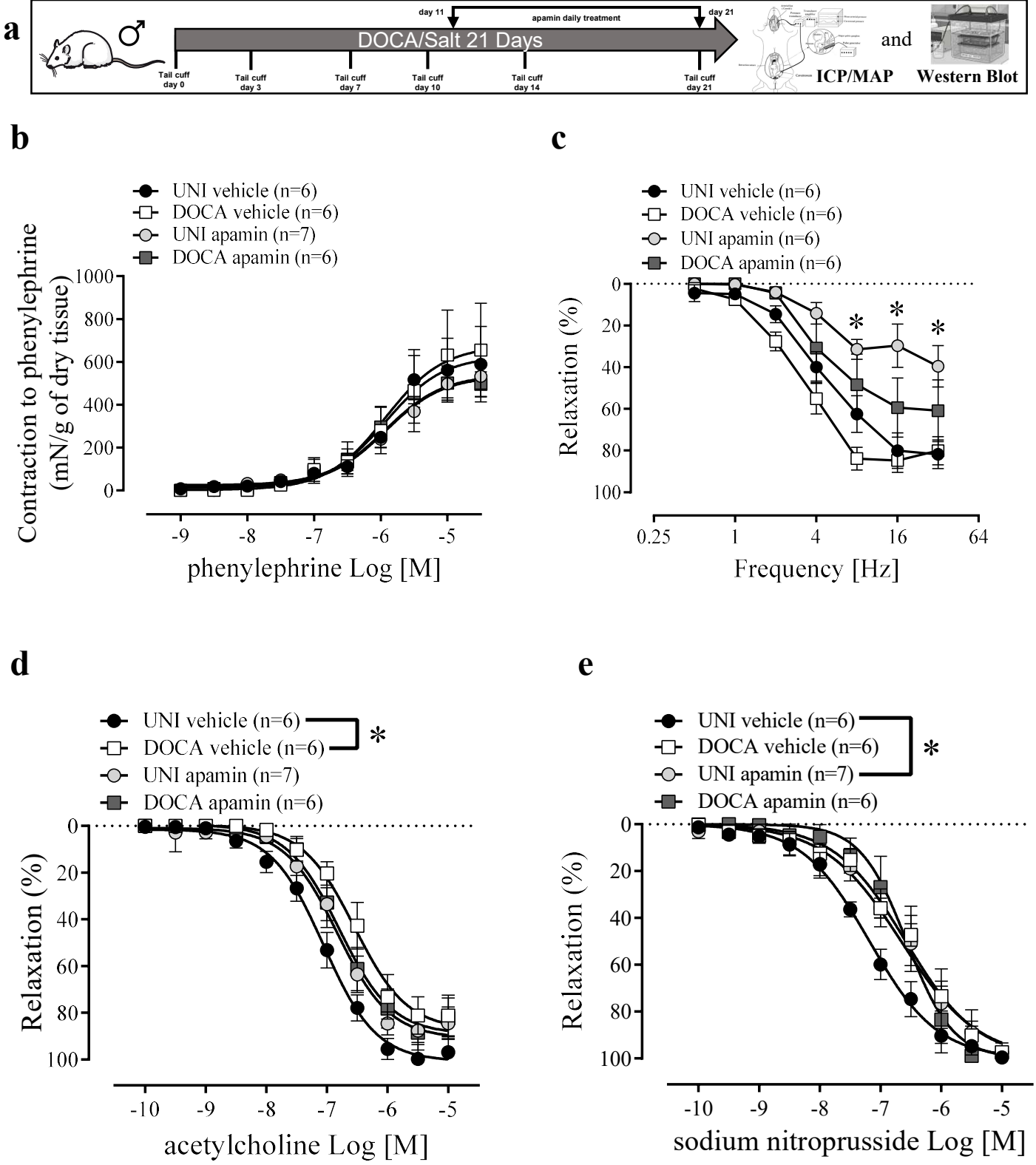
a
day 11
apamin daily treatment
day 21
DOCA/Salt 21 Days
Tail cuff day 0
Tail cuff day 3
Tail cuff day 7
Tail cuff day 10
Tail cuff day 14
Tail cuff day 21
and
ICP/MAP
Western Blot
b
UNI vehicle (n=6)
DOCA vehicle (n=6)
UNI apamin (n=7)
DOCA apamin (n=6)
Contraction to phenylephrine (mN/g of dry tissue)
phenylephrine Log [M]
c
UNI vehicle (n=6)
DOCA vehicle (n=6)
UNI apamin (n=6)
DOCA apamin (n=6)
Relaxation (%)
Frequency [Hz]
d
UNI vehicle (n=6)
DOCA vehicle (n=6)
UNI apamin (n=7)
DOCA apamin (n=6)
Relaxation (%)
acetylcholine Log [M]
e
UNI vehicle (n=6)
DOCA vehicle (n=6)
UNI apamin (n=7)
DOCA apamin (n=6)
Relaxation (%)
sodium nitroprusside Log [M]